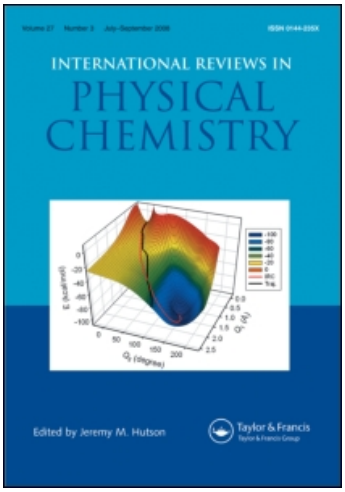

International Reviews in Physical Chemistry
Publication details, including instructions for authors and subscription information:
http://www.informaworld.com/smpp/title~content=t713724383

Transition Metal Dichalcogenides and Their Intercalates

E. A. Marseglia[a]
[a] Physics and Chemistry of Solids, Cavendish Laboratory, Cambridge, UK

To cite this Article Marseglia, E. A.(1983) 'Transition Metal Dichalcogenides and Their Intercalates', International Reviews in Physical Chemistry, 3: 2, 177 — 216
To link to this Article: DOI: 10.1080/01442358309353343
URL: http://dx.doi.org/10.1080/01442358309353343

International Reviews in Physical Chemistry (1983), *3* (177–216)

TRANSITION METAL DICHALCOGENIDES AND THEIR INTERCALATES

E.A. MARSEGLIA

Physics and Chemistry of Solids, Cavendish Laboratory, Madingley Road, Cambridge, UK

ABSTRACT

The transition metal dichalcogenides form a group of layered, highly anisotropic compounds which exhibit interesting and unusual physical properties. Compounds formed from the Group IV, Group V and Group VI transition metals and from sulphur or selenium have been the subject of a great deal of interest in the past few years because of the possibility of introducing foreign species between the layers and causing many of the properties of the host lattice to change in a predictable way, consistent with the rigid band model. The most common intercalate complexes are those formed from alkali metals, Lewis bases and transition and post-transition metals. In this review a number of these compounds are discussed, with special emphasis on those which provide new information about the host material, or where some new, interesting property of the complex has been demonstrated.

INTRODUCTION

The transition metal dichalcogenides (TMDC) of interest in this review are formed from sulphur or selenium atoms (denoted by X), and the transition metals (T) of the Group IV, V and VI elements in the ratio TX_2. These TX_2 compounds are found with layered structures in which sandwich layers of strong covalently bound TX_2 units are separated by a so-called 'van der Waals' gap. That is, the bonding between the sandwiches is weak and may include van der Waals forces, although weak electrostatic forces must also be involved. In these layered structures, atoms of one kind lie on hexagonal lattice planes, and the chalcogen planes are stacked in close-packed arrangements with the metal atoms fitting into interstitial positions between every *other* chalcogen plane. The choice of layer stacking can lead to a rich variety of possible polytypes. If we denote the chalcogen atom layers by capital letters and metal atom layers by lower-case letters, the five most common polytypes are:

1T	AcB	AcB	. . . .	
3Ra	AcB	CbA	BaC	. . .
2Ha	BaB	CaC	BaB	. . . .
2Hb	CbC	BcB	CbC	. . . .
3Rb	AcA	BaB	CbC	AcA . . .

where the letters refer to the three inequivalent positions marked in *Figures 1 and 2*. Note

0144–235X/83/02 0177–40 $03.00

that in the 2Ha and 1T structures the metal atoms are stacked directly above each other while in the other polytypes given here the metal atoms are staggered. In both the 2H structures, the metal atom is surrounded by chalcogen atoms in trigonal prismatic coordination (TP), while in the 1T structure, the coordination is trigonal antiprismatic, (TAP), which is essentially octahedral with a c/a ratio of ~ 1.7 (*see Figure 1b*). The 3R structure can have either TP or TAP coordination. These differences in coordination lead to important differences in electronic structure as we shall see in the next section.

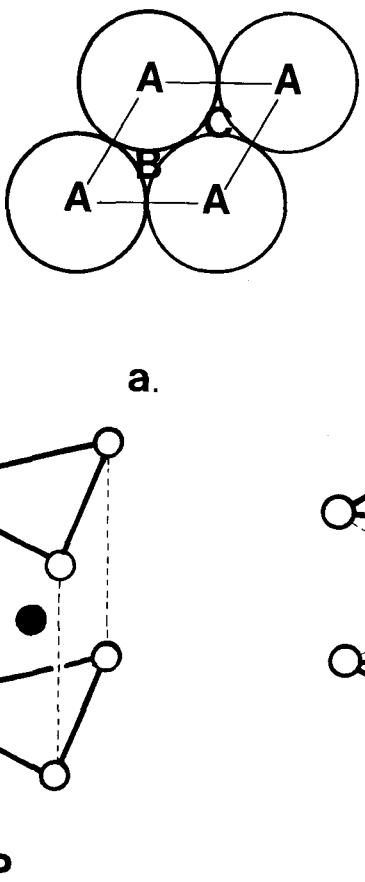

FIG. 1. (a) Schematic arrangement of a close packed layer of atoms. The atoms of the next layer can lie with their centres at either position B or C. (b) Trigonal prismatic (TP) and trigonal antiprismatic (TAP) coordination.

The crystallographic axes for the 1T and 2H compounds are those for a standard hexagonal system with a and b parallel, and c perpendicular, to the layers. Typical values are 3–4 Å for the a parameter and 6 Å for the inter-sandwich separation. The unit cell for the 3R structure is rhombohedral, but from the projection given in *Figure 2*, we see that it is very closely related structurally to the other polytypes.

The formation of layered structures is characteristic of compounds with highly polarizable ions where the asymmetric coordination of the anions is stabilized by the polarization energy (Haas, 1982). Further stabilization can be acquired by slight distortions

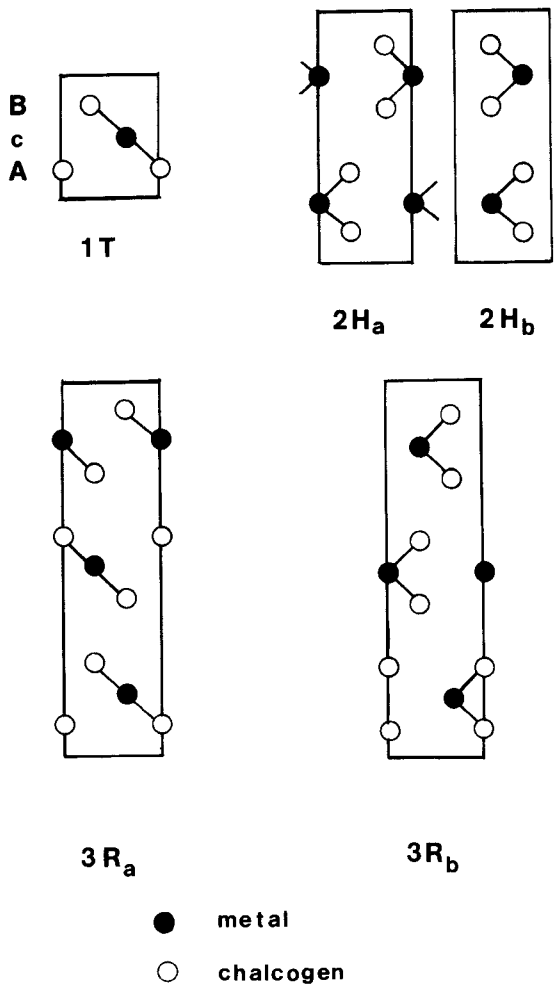

FIG. 2. $11\bar{2}0$ sections of the 1T (1 layer/unit cell; trigonal symmetry), 2H (2 layers/unit cell; hexagonal symmetry) and 3R (3 layers/unit cell; rhombohedral symmetry) polytypes found in the transition metal dichalcogenides. A,B,c refer to the relative positions of the layers — *see Figure 1a* and text.

of the basic structure, and indeed, distorted TX_2 layer structures are often found, usually those containing the highly polarizable Te ions (e.g., $MoTe_2$, WTe_2, $NbTe_2$, $TaTe_2$ and VTe_2) (*see*, for example, Brown, 1966; Clarke *et al.*, 1978). However, anion polarization is not the only mechanism which can contribute to a lattice distortion and we shall discuss examples later of structural changes where electron–phonon (vibronic) interactions and metal–metal interactions are also important.

The presence of a weakly bound van de Waals gap has a number of interesting consequences. Firstly, the TX_2 compounds show very anisotropic properties. For example, the Raman active vibrational frequencies for modes (phonons) which involve intralayer chalcogen–chalcogen bonding are many times higher than the so-called layer–layer modes, which involve bonding across the gap (*see Figure 3*) (Bagnall *et al.*, 1980). The compressibility of these materials is highly anisotropic, as seen by changes of lattice parameter and

vibrational frequencies under hydrostatic pressure (Bagnall *et al.*, 1980, 1983). Anisotropy is also observed in optical and transport properties (Edwards and Frindt, 1971; Hambourger and Di Salvo, 1980; Bayliss and Liang, 1982). The most important consequence of the van de Waals gap for the present discussion, however, is the relative ease with which the layers can be separated, allowing 'guest' species to diffuse in and out of the gap of the 'host' material. This process is known as intercalation and was first observed by the Chinese in $\sim$ 700 BC in the swelling of layered clay minerals by intercalation of water. Interest in the process has accelerated in the past ten years because of potential applications in catalysis and solid-state batteries and, more fundamentally, because of the possibilities it presents of varying physical properties in a controlled way, making it a powerful analytical technique for studying the properties of host and product alike.

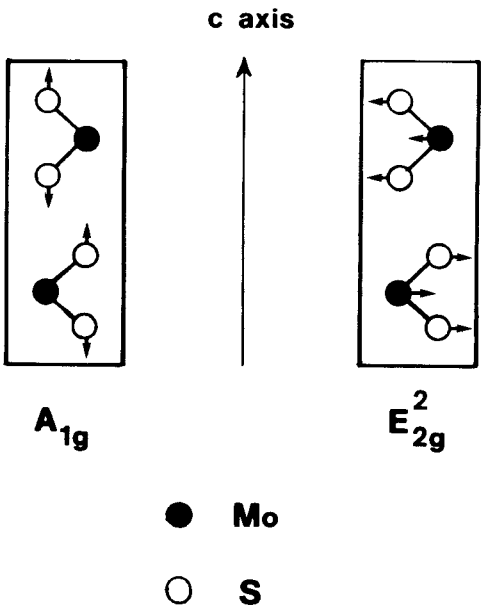

FIG. 3. A_{1g} and E^2_{2g} (layer–layer) Raman active vibrational modes in 2H–MoS_2.

Intercalation in transition metal dichalcogenides usually involves a transfer of electrons from the guest intercalate to the unoccupied transition metal d band of the host. The subsequent Coulombic attraction between the cation thus formed and the negatively charged layer is the main driving force for this reaction. With one possible exception (*see* p. 198), only electron donor 'guest' species are known to intercalate between the TX_2 layers, the most common being alkali metals, Lewis bases, transition metals and post-transition metals. For electron acceptors, the charge distribution over the layers would be energetically much more unfavourable, because both the intercalate ion and the neighbouring chalcogen layers would be negatively charged (*Figure 4*). The mechanism and kinetics of intercalation in transition metal dichalcogenides have been reviewed elsewhere (Acrivos, 1979). Suffice it to say here that the steps probably involve adsorption onto the surface of the crystal, formation of an activated complex which opens up the layers, then rapid diffusion around the edge and entry into the gap between the layers. A number of general reviews on both the chemistry and physics of intercalation have also appeared recently (Gamble and Geballe, 1975; Whittingham, 1978a; Levy, 1979; Rouxel, 1980; Friend, 1982; McEwan and Sienko,

1982a; Pietronero and Tosatti, 1982; Whittingham and Jacobson, 1982; Yoffe, 1982). In the present review we shall only be concerned with a few important aspects of the intercalation of the transition metal dichalcogenides, and in particular, will focus on those examples where a study of the intercalation complex has provided information about the properties of the host material, or where some new interesting property of the complex has been demonstrated. For simplicity, intercalation complexes will be denoted as M_xTX_2, where M = guest intercalate, T = transition metal, X = sulphur or selenium and x = fractional composition.

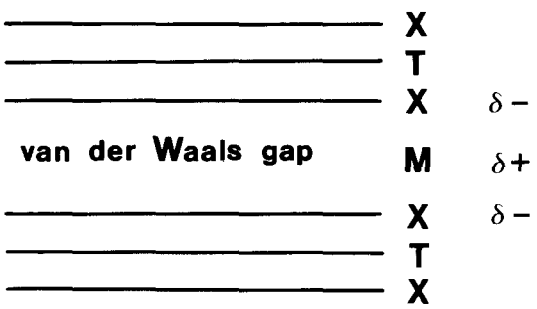

FIG. 4. Schematic picture of an intercalation complex MTX_2, where M is an electron donor. The M atoms can occupy tetrahedral, octahedral or trigonal prismatic sites in the gap.

Band scheme and rigid band model

Intercalation can best be understood by looking at the electronic structure of the host transition metal dichalcogenides. *Figure 5* shows the energy band schemes for the Group IV, Group V and Group VI dichalcogenides which were first proposed by Wilson and Yoffe (1969), and which have since been confirmed by band structure calculations and by a number of physical measurements, including spectroscopic data, photoemission, electron energy loss and transport measurements (Bell and Liang, 1976; Friend *et al.*, 1977a; Mattheiss, 1973).

From *Figure 5* we see that the valence band is based predominantly on the overlap of the s and p orbitals of the chalcogen atoms, and the conduction band is based predominantly on the overlap of transition metal d orbitals, although a more accurate description is in terms of complex hybridized bands. For the Group IV materials, the four valence electrons per metal atom just fill up the valence band and a semiconductor results (or a semimetal if there is partial p–d overlap). The semiconductor band gap is of the order of 1–2 eV. The Group V materials are all metallic, since there is an extra electron which partially populates the conduction band. There are two types of conduction band depending on the crystal field which results from octahedral or trigonal prismatic coordination. The octahedral environment causes the usual splitting into e_g and t_{2g} levels, with a slight further splitting of the t_{2g} level into a doublet and singlet state due to the antiprismatic distortion. Orbital overlap then results in a d-conduction band which is approximately 7 eV wide. In the trigonal prismatic case, the crystal field splitting results in a lower level which, upon band formation, is separated from the other d bands by a small energy gap. (This lower level is commonly known as the 'd_{z^2}' band, although it is more accurately a hybridized state.) The lowering of energy of an occupied 'd_{z^2}' band helps to stabilize the trigonal prismatic structure against the repulsive Madelung energy resulting from shorter chalcogen–chalcogen distances. Thus,

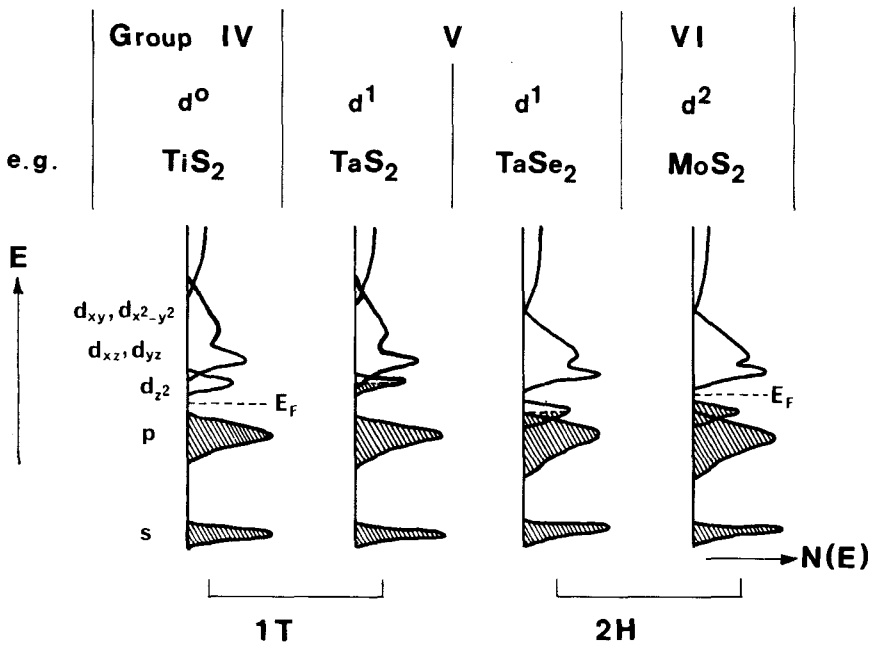

FIG. 5. Band schemes for the transition metal dichalcogenides showing energy (E) versus the density of electron states, $N(E)$. (After Bell and Liang, 1976, and Wilson and Yoffe, 1969.) E_F = Fermi energy; s,p,d refer to dominant orbital character of hybridized bands.

since the conduction band is empty in the Group IV compounds, only the 1T structure exists. The structures of the Group V compounds, however, depend critically on whether the band structure energy or the Madelung energy is greater and both types of coordination are observed. The Group VI compounds are mainly of the 2H-type since they have two electrons per formula unit in the d_{z^2} band which lower the band energy enough to overcome the Madelung energy. Since this d_{z^2} band is now filled, the Group VI disulphides and diselenides are semiconductors, and we would expect intercalation to be very difficult in these materials since transferred electrons must go into the higher energy d states.

In studying the transport properties of conducting materials it is useful to know how the charge carriers (either electrons or holes) are able to move through the crystal. This depends on the symmetry of the material and is intimately related to the shape of the Fermi surface. This is a constant energy surface drawn in reciprocal space connecting the most energetic occupied electron states in the material (i.e., states at the Fermi level). Most carrier scattering processes only involve stages very close to the Fermi level and so it is these states which determine the transport behaviour. *Figure 6* shows the shape of the Fermi surface in both 1T and 2H materials (Mattheiss, 1973; Wilson *et al*, 1975). The dotted lines in 6b indicate how the size of the electron and hole pockets are changed upon intercalation, i.e., upon addition of electrons. In the 2H Group V materials, with one d electron per formula unit, the conduction band is half-filled, and in this case the free carriers are positive holes. Thus, when electrons are added to the band the number of holes, and hence the number of free carriers, is decreased, so we would expect the conductivity of Group V–2H compounds to *decrease* upon intercalation. The conductivity of Group IV and Group VI compounds should *increase* upon intercalation because electrons are being added to an empty band.

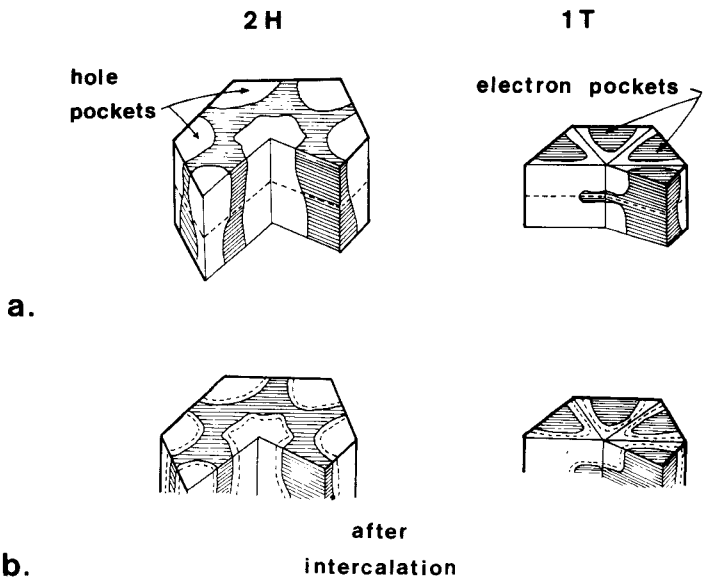

FIG. 6. Schematic Fermi surfaces in reciprocal space for the 1T and 2H structures (a) before and (b) after intercalation. Shaded areas are occupied by electrons.

The important parameters that are derived from the transport measurements mentioned in this review are the Hall coefficient, which gives an indication of the number and type of charge carriers, and the resistivity, which can yield the number of charge carriers, and from its temperature dependence, the mechanisms that are responsible for scattering the carriers and affecting their mobility. Also, the Pauli paramagnetic susceptibility gives information about carrier numbers in metals.

There is some reason to believe, both from band structure calculations and from experiment, that there are only very small changes in the shape of the host metal d bands when the *c* axis is expanded (Mattheiss, 1973), or when intercalate species are introduced into the van der Waals gap (Clark, 1976; McCanny, 1979; Acrivos *et al.*, 1981). Thus to a first approximation we can consider that the only change introduced upon intercalation is the increased occupancy of the band. This is known as the rigid band model, and is a very useful concept particularly for explaining the electronic properties of intercalation complexes (Friend, 1982; Yoffe, 1982). We shall now examine the transition metal dichalcogenides and their intercalates in more detail, in the order Group IV, Group V and Group VI, and shall see how the behaviour of each is very much determined by the underlying electronic structure we have just discussed.

GROUP IV

TiS_2

The Group IV dichalcogenide, TiS_2, has proved to be a controversial material because it exhibits rather unusual conducting behaviour at all temperatures, no matter how carefully prepared to eliminate any impurities which might contribute to the conductivity. The question has arisen as to whether it is a true semimetal, with p–d overlap, or an extrinsic semiconductor. Band structure calculations have added to the confusion in that five have predicted a semiconductor with band gaps ranging from 2 to 0.3 eV (for references *see*

Klipstein *et al.*, 1981), and two have predicted partial p–d orbital overlap, giving a semimetal (Benesh *et al.* 1983; Temmerman *et al.*, 1982). Recent experimental evidence, however, has convincingly supported an extrinsic semiconductor model with a band gap of ~ 0.12 eV, the carriers being derived from interlayer Ti atoms, some of which may have been displaced from the TiS_2 sandwich to the van der Waals gap (Friend *et al.*, 1977a; Logothetis *et al.*, 1979; Chen *et al.*, 1980; Klipstein *et al.*, 1981; Barry *et al.*, 1983; Klipstein and Friend, 1983a). In fact, transport measurements under hydrostatic pressure have demonstrated that it takes 40 kbar of pressure to cause the p–d bands to overlap partially and form a semimetal (Klipstein and Friend, 1983a).

In addition, the resistivity of TiS_2 shows a strong, unexpected temperature dependence between 20 and 400 K (Thompson, 1975b) varying approximately as T^2 rather than with the more usual linear dependence expected for a normal metal. This unusual behaviour has been explained by a mechanism whereby the electrons are scattered, not only within pockets of the Fermi surface but also between pockets by mainly acoustic phonons at low temperatures (Klipstein *et al.*, 1981). Strong coupling between electrons and phonons occurs quite commonly in these TMDC compounds and, as we shall see, can lead to a number of interesting effects.

TiS_2 can be intercalated by all the alkali metals, but, by far, Li intercalation has been the most studied because of the potential interest of the $LiTiS_2$ system as a high energy density solid state battery. The preparation and structural and electrochemical properties of this system have been covered extensively in the above mentioned reviews. Intercalation is extremely fast and there appears to be a single phase from TiS_2 to $LiTiS_2$ with smoothly varying lattice and thermodynamic parameters. The small Li atom fits easily into the octahedral interstices between the layers and only a small c axis expansion, $\sim 5\%$, is observed. A band structure calculation for $LiTiS_2$ by McCanny (1979) shows that the main modifications on introducing lithium are far removed in energy from the valence and conduction band edges. This result provides support for the use of the rigid band model, especially for interpreting transport properties. In fact the calculation shows less dispersion in the p_z sulphur bands in the intercalation complex, indicating that the presence of the lithium may weaken the covalent bonding within the layers. This idea is supported by the fact that in TiS_2 and $TiSe_2$ the a axis expands upon Li intercalation in contrast to other less covalent layered compounds which show a contraction.

The lithium atoms in $LiTiS_2$ are highly mobile within the layers, in fact, the diffusion coefficient is the highest known for any lithium compound at room temperature, and even so, diffusion is the rate determining step in the intercalation reaction (Chianelli *et al.*, 1978). The activation energy for the diffusion of the Li ion is 0.1 eV and the ionic conductivity is 10^{-3} to $10^{-4}\,(\Omega\,\mathrm{cm})^{-1}$. The Li atoms also appear to order at room temperature in the system Li_xTiS_2 for certain values of x. High resolution electrochemical experiments have indicated the presence of this ordering from the inverse derivative of the cell EMF which shows peaks at $x = 1/9, 1/4, 5/7, 4/5$ and $6/7$ (Thompson, 1978). However, these peaks should be treated with some caution, since the structure of the EMF curve also depends on other factors not associated with lithium ordering. More direct evidence comes from diffuse X-ray scattering which shows very weak $2a$ and $3a$ superlattice formation for $x = 1/4$ and $x = 1/3$, respectively (Hibma, 1980b; Hallak and Lee, 1983). On the other hand, Kleinberg *et al.* (1982) have carried out experiments on the ^{7}Li NMR linewidths of $Li_{1/3}TiS_2$, and have found that the second moment, which is very sensitive to short-range arrangements of the ^{7}Li nuclei, is not consistent with a simple ordered superlattice and suggests a more complicated arrangement of Li ions.

Evidence that the metal outer s electron of the Li atom is transferred to the host d band can be seen, for example, in the absence of the Li^7 Knight shift, which measures s electron overlap with the Li nucleus (Silbernagel and Whittingham, 1976), in the behaviour of the

magnetic susceptibility (Murphy *et al.*, 1976) and in optical transmission experiments (Beal and Nulsen, 1981a,b). Transport measurements show that the charge transfer leads to metallic behaviour as we would expect from the rigid band model (Onuki *et al.*, 1981; Klipstein and Friend, 1983b). *Figure 7*, for example, gives the variation of the resistivity with temperature for various samples of Li_xTiS_2. Carrier concentrations determined from the Hall coefficient are indicated by each curve (Klipstein and Friend, 1983b). For a carrier concentration of 2×10^{22} cm^{-3}, corresponding to the formula $LiTiS_2$, the resistivity is decreased by almost two orders of magnitude below that of the unintercalated material.

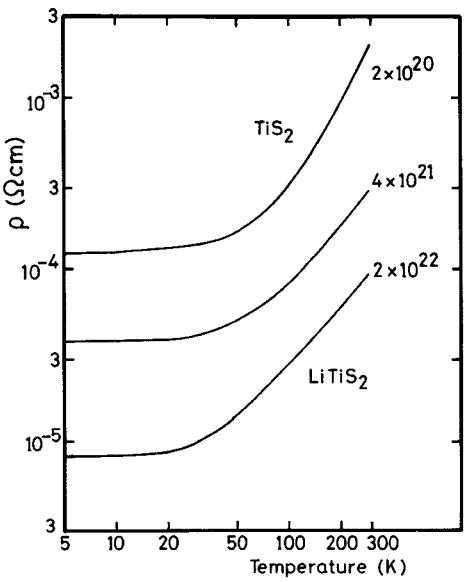

FIG. 7. Variation of resistivity with temperature of TiS_2 and Li_xTiS_2, where $x \cong 0.25$ and 1.0, respectively (Klipstein and Friend, 1983b).

Structural studies on Na_xTiS_2 have shown that unlike Li_xTiS_2, at least three different phases exist between $x = 0.0$ and $x = 1.0$ (Rouxel *et al.*, 1971). These phases can be characterized by the fractional number of intercalated van der Waals gaps (stages) and the coordination of the intercalate ion, which may be distorted octahedral (TAP) or trigonal prismatic (TP). Thus, in $Na_x\,TiS_2$, the phases are a Stage II compound ($0.17 < x < 0.33$) where Na^+ ions occupy every other layer, a Stage I (TP) compound ($0.38 < x < 0.68$) where sodium has trigonal prismatic coordination in every layer, and a Stage I (TAP) compound ($0.79 < x < 1.0$) where sodium is in a distorted octahedral site in every layer *(see Fig. 8)*. In fact, all the noble and alkali metal intercalates (except lithium) of the Group IV transition metal dichalcogenides show evidence of this staging behaviour, the highest reported being Stage IV (Wiegers, 1980). Obviously, the relative stability of two different stages with the same overall composition depends on

1. The effective interaction between the intercalate ions within the same layer and in different layers.
2. The energy required to separate the layers.

Thus, Hibma (1982) concludes that higher stage compounds should occur only if the alkali ions have trigonal prismatic coordination. His argument is that the bonding between

chalcogen atoms across the van der Waals gap for the octahedrally and tetrahedrally coordinated intercalates is not very different from the bonding in the host material, because the alkali ions are small and the chalcogen atoms are still essentially close packed. It is only in the case of trigonal prismatic coordination that the difference in chalcogen ion bonding across a non-intercalated and an intercalated layer is sufficiently large to balance the increased repulsion between the intercalate ions in the higher stage compounds. Trigonal prismatic coordination is usually found for the larger alkali metal complexes which are fully or nearly fully intercalated, such as $KTiS_2$, $RbTiS_2$ and $CsTiS_2$, and staging is indeed found in these materials. It is also interesting to note here that from a structural point of view trigonal prismatic coordination should be the most favourable for ionic conduction in these layered intercalate complexes; indeed, diffusion coefficients for trigonal prismatically coordinated sodium ions seem to be considerably larger than those for octahedrally coordinated sodium (Whittingham, 1978a).

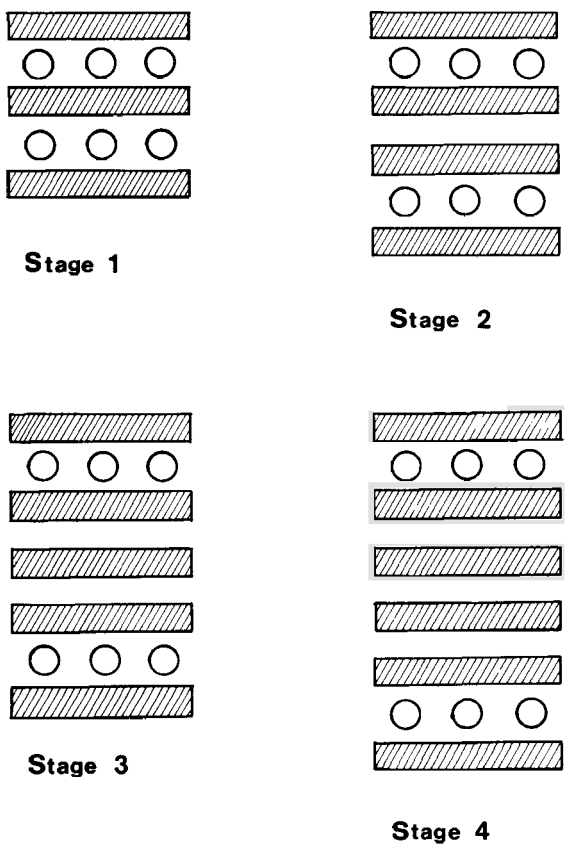

FIG. 8. Schematic diagram of staging in a layer compound. For low intercalate concentrations, only one out of n gaps is filled. Such a compound is said to be of stage n.

Hibma (1980c) has also studied the ordering of the Na ions in Na_xTiS_2 using X-ray techniques. Four types of superstructures have been found at room temperature at $x = 1/8$, $1/6$, $1/2$, $3/4$. For stoichiometries deviating from these values additional diffuse scattering is seen due to partial disordering. The stability of a particular ordered structure must depend on

interactions between the sodium ions, and on interactions with the host lattice. Hibma has shown that interactions between the Na ions decrease much faster with interionic distances than a simple Coulomb law would predict, due to the strong screening of the Coulombic interactions by the conduction electrons of the host.

Recently, attention has been directed to the silver and copper intercalates of TiS_2, and to their possible use as solid state batteries. Although these noble metal-based batteries only show $\sim 1/10$ of the EMF of the lithium batteries they can be constructed with the advantage of using aqueous electrolytes (Scholz *et al.*, 1980). Ag intercalated into TiS_2 occupies octahedral sites and has a diffusion activation energy of 0.4 eV (Scholz and Frindt, 1980). It is not known yet whether or not the Ag is completely ionized to Ag^{+1} but it can perhaps be inferred by analogy to Cu_xTiS_2, where it is thought from susceptibility and transport measurements that the Cu is present as Cu^{+1} (Le Nagard *et al.*, 1975; Schöllhorn, 1982a). Also, recent resistivity experiments on Ag intercalated into $NbSe_2$ are consistent with a +1 charge on the Ag ion (Rogers, 1982). Low temperature ordering of the Ag ions in $Ag_{0.33}TiS_2$ has been observed using X-ray diffraction (Ünger *et al.*, 1978; Suter *et al.*, 1982). At 170 K, the line shapes of the sharp $3a \times 3b$ superlattice peaks due to the ordered phase begin to broaden and this continues gradually to 260 K, where a second-order transition takes place to the disordered phase. An order–disorder transition of this type is known as 'superlattice melting' as it shows some similarities to a normal solid–liquid transition. The difference in this case is that it is second order, taking place continuously over a very large temperature range (~ 100 degrees). This is allowed because the high temperature 'fluid' phase is not isotropic but has a symmetry imposed by the host crystal (*see* Bak, 1980). In contrast, the Cu ions in $Cu_{0.70}TiS_2$, which occupy tetrahedral sites, show no sign of ordering at low temperatures, at least from magnetic and transport studies (Le Nagard *et al.*, 1975).

Nonstoichiometric TiS_2, i.e., $Ti_{1+x}S_1$, can be considered as a case of self-intercalation, with the excess Ti ions occupying octahedral sites within the van der Waals gap. Electron diffraction studies of this system have shown that at certain values of x, superstructures are observed, indicating ordering of Ti intercalate ions (Moret *et al.*, 1977, 1978). It is interesting to note also that the complex $Ti_{1/3}TiS_2$ cannot be further intercalated with alkali metal ions (Rouxel, 1980), perhaps because diffusion is inhibited by the presence of the Ti ions, which are ordered on octahedral sites and which may cause the layers to be more tightly bound. Of course, complete intercalation of Ti into TiS_2 leads to the compound TiS which has the NiAs structure, and is a completely isotropically bound system.

TiS_2 does not seem to intercalate larger guest species very easily and this may be due to displaced metal ions between the layers which always seem to be present in this material. These highly charged ions would considerably increase the energy required to open the interlayer space. Early failures to intercalate TiS_2 directly with pyridine or substituted pyridines have been associated with this deviation from stoichiometry and even when highly stoichiometric TiS_2 was finally intercalated with 2,4,6 trimethyl pyridine it took 30 days at 300°C (Thompson *et al.*, 1975).

$TiSe_2$

$TiSe_2$ is the one exception to the Group IV TS_2 and TSe_2 compounds in that it is a semimetal with positive carriers (holes) (Friend *et al.*, 1977b). That is, the valence (p) and conduction (d) bands overlap partially so that electrons from the valence band can enter the conduction band and metallic behaviour is observed. This is shown schematically in reciprocal space in *Figure 9a*. Intercalation of Li into $TiSe_2$ causes it to change to a normal metal with n-type carriers (electrons), with the resistivity of Li_xTiSe_2 decreasing with increasing x as expected (Klipstein and Friend, 1983b). However, the transport measurements show that some holes may still be present in $LiTiSe_2$, perhaps casting doubt on the validity of the rigid

band model in this case. This idea of a changing band structure in Li_xTiSe_2 has also been predicted from calculations by Temmerman (1983), and may explain why the magnetic susceptibility of $LiTiSe_2$ (Murphy *et al.*, 1976) was higher than that expected from the rigid band model, i.e., more free carriers are present than the model would predict.

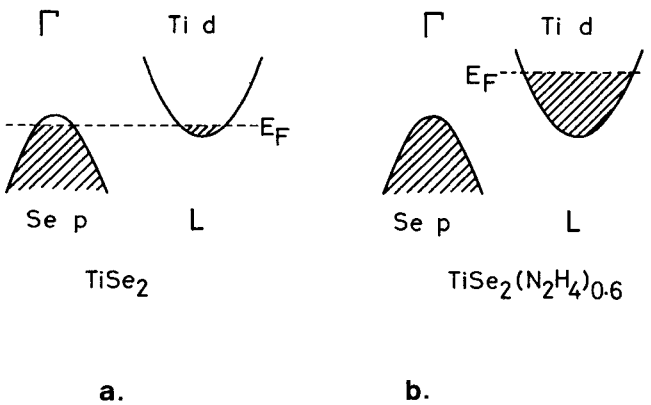

FIG. 9. (a) Band scheme for $TiSe_2$, showing the small p–d band overlap. At the symmetry point Γ, the free carriers are holes, and at L they are electrons. (b) Band scheme for $TiSe_2(N_2H_4)_{0.6}$ showing the greatly increased occupation of the Ti d band as a result of electron transfer of 0.45 electrons per $TiSe_2$ formula unit from the hydrazine (Friend, 1982).

$TiSe_2$ is the only Group IV diselenide or disulphide that undergoes a structural distortion at low temperatures. The transition takes place at 200 K causing both the *a* and the *c* lattice parameters to double (Di Salvo *et al.*, 1976). This change in crystal structure has the effect of coupling the holes in one part of reciprocal space to the electrons in another part (*see Fig. 9a*). This, in turn, decreases the number of carriers by a factor of about 10 causing an anomaly in the temperature dependence of the resistivity, although the system is still metallic below the transition. It has been suggested that this electron-hole coupling is a driving force for the distortion (Di Salvo *et al.*, 1976; Wilson, 1978b; Gaby *et al.*, 1981). If this were true, we would expect any change in the filling of the bands to affect sensitively the distortion temperature. Experiments with hydrazine intercalation of $TiSe_2$ show that this does not happen. By adding hydrazine up to $\sim$ 15%, the hole pockets at the top of the p band in $TiSe_2$ can be completely filled, giving a charge of + 0.75 per N_2H_4, but there is no change in the temperature of the distortion (Sarma *et al.*, 1982a). It is more likely therefore that the transition can be better described by an instability in one of the vibrational modes, known as a soft phonon transition. In fact, a softening of the transverse optic phonons as a function of temperature has been observed in $TiSe_2$ by inelastic neutron scattering (Moncton *et al.*, 1978). Also, the p–d overlap in $TiSe_2$ is slight, so that the number of carriers that would be involved in a structural transition is actually quite small, and it is questionable that changes in electron energies below the transition would be sufficient to drive the distortion.

The situation for higher concentrations of N_2H_4 in $TiSe_2$ is less clear, since no resistive anomaly at all was observed in the temperature dependence of $TiSe_2(N_2H_4)_{0.6}$ (Sarma *et al.*, 1982b). However, a fall in the Pauli susceptibility was seen below 150 K, indicating a loss of electrons, and perhaps indicating the presence of a very weak structural transition (Guy *et al.*, 1982a). A similar fall in Pauli susceptibility is seen in $LiTiSe_2$ below 40 K (Murphy *et al.*, 1976), which may be related to a weak anomaly observed in the transport behaviour of $LiTiSe_2$ at $\sim$ 50 K (Klipstein and Friend, 1983b).

The question of the nature of the transition in $TiSe_2$ becomes even more intriguing when we consider the effect of doping $TiSe_2$ with small amounts ($\sim$ 1–3%) of Ta or V, which are thought to be present substitutionally but may also be present in interlayer sites. The main effect of this doping is to alter the free carrier concentration in the conduction band, and it is found that the transition temperature in this case *is* suppressed, at a rate of 18 K/at% (Di Salvo and Waszczak, 1978). However, addition of up to 4% hydrazine to $V_{0.01}Ti_{0.99}Se_2$ did not change the host transition temperature. Instead, the size of the transport anomaly associated with the distortion decreased with increasing hydrazine concentration and vanished for concentrations in excess of 13% (Sarma *et al.*, 1981). In the case of excess Ti in the compounds $Ti_{1+x}Se_2$ where the excess metal occupies interlayer sites the transition temperature is also suppressed by 35 K/at %. Interestingly, the periodicity of the distortion remains unchanged (Woo *et al.*, 1976). As we shall see later, the periodicity of the distortion in the Group V layered materials is very sensitive to electron concentration.

Another effect of this doping and partial self-intercalation is to create considerable disorder in these crystals, and it may be this effect that is lowering the distortion temperature, rather than the change in carrier concentration which does not correlate in any simple way with the depression of the distortion temperature (Di Salvo and Waszczak, 1978). Clearly, further studies, particularly structural measurements, are needed before the distortions in $TiSe_2$ and its intercalates are completely understood.

At very low temperatures the resistivity of V-doped $TiSe_2$ rises sharply, indicating non-metallic behaviour *(see Fig. 10)*. We know that the structural distortion has removed some of the free carriers from the conduction band, and it is thought that local moments which form on the V atoms must remove most of the remaining carriers (Guy *et al.*, 1982a). The carriers are now so reduced in number that they become sensitive to the random potentials caused by the substitutional V atoms, and localize at low temperatures, hence, the non-metallic behaviour. The theory for this localization of electrons by random potentials was first investigated by Anderson (1958), and is usually named after him (*see also* Mott, 1974). The localization in V-doped $TiSe_2$ can be completely removed by intercalation with hydrazine *(Fig. 10)*, because now the increased carrier concentration once again screens out the impurity potentials of the V (Sarma *et al.*, 1982b). The extra carriers in the 1% and 3% V-doped $TiSe_2(N_2H_4)_{0.6}$ also cause an increase in the Pauli paramagnetism on intercalation and a decrease in the size of the average V moment (Guy *et al.*, 1982a). A possible interpretation might be that the V is distributed between interlayer and substitutional intralayer sites with local moments in both cases, and only the intralayer moments are destroyed upon intercalation. The latter effect could come about because the extra carriers which have been transferred to the conduction band screen out the localization potential of the V atoms, causing the spins to become delocalized. In this model, the V atoms between the layers retain their local moments, and assuming this V is present as V^{+3} with a spin only moment of 2.83 (*see* Parkin and Friend, 1980a,b) it can be estimated that approximately one quarter of the V atoms present occupy the interlayer sites (Guy *et al.*, 1982a).

Zirconium and Hafnium Dichalcogenides (S, Se)

The zirconium and hafnium diselenides and disulphides are all medium-to-large band gap semiconductors with small extrinsic electron concentrations and, like TiS_2, they do not seem to undergo any lattice distortions at low temperatures. ZrS_2 and HfS_2 are transparent red crystals in their pure state, and when they are intercalated with Li they become opaque and highly reflecting due to the presence of the conduction electrons donated by the Li atoms. Optical transmission measurements on these materials also illustrate this transfer of electrons very clearly. *Figure 11* shows the transmission spectrum of HfS_2, both before and after intercalation (Beal and Nulsen, 1981a). At low energies a rise in the absorption edge

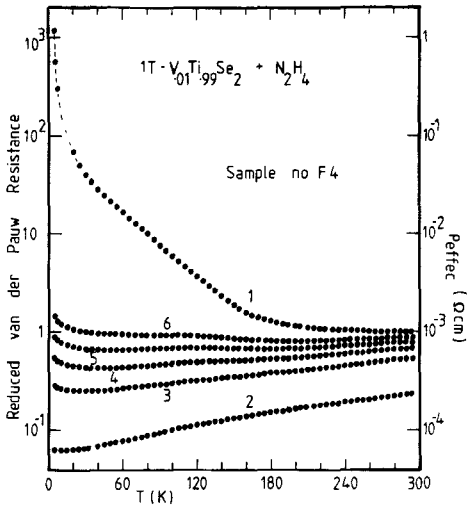

FIG. 10. Effective resistivity versus temperature for $V_{0.01}Ti_{0.99}Se_2$ before and after intercalation with hydrazine and at different stages of deintercalation. Numbers indicate the order of experiments: (1) pure $V_{0.01}Ti_{0.99}Se_2$(2) completely deintercalated, (3)–(6) partially intercalated phases (Sarma *et al.*, 1982b).

(A) is seen on intercalation which is due to the presence of the free carriers. This rise comes from the excitation by the light of collective free carrier oscillations known as plasmons and is called the Drude edge. Note also that the fundamental absorption edge at $\sim$ 2eV(B) in HfS_2 is not a sharp transition. This is because the maximum in the valence band and the minimum in the conduction band are at different points in reciprocal space, and optical transitions across this gap can only be indirect, i.e., phonon assisted to conserve momentum. Upon intercalation with Li, the gap remains indirect, but is shifted to higher energies by $\sim$ 0.5 eV. After the fundamental edge there is a broad shoulder due to transitions within the d_{z2} band, and in $LiHfS_2$ we see that this broad shoulder is decreased because the number of states available for transitions is reduced as electrons are added to the band.

Transport measurements on ZrS_2 and $ZrSe_2$ have revealed interesting differences in the conducting behaviour of these materials (Conroy and Park, 1968; Onkui *et al.*, 1982a; Klipstein, 1982). ZrS_2 and $ZrSe_2$ always appear to grow with an appreciable extrinsic electron concentration, which may be due, as in TiS_2, to displacement defects, that is, metal atoms displaced from within the layer to interlayer sites (Takeuchi and Katsuta, 1970; Wilson, 1978a; Klipstein, 1982). However, at low temperatures ZrS_2 becomes insulating, indicating that carrier localization is taking place, while $ZrSe_2$ remains metallic at all temperatures. $ZrSe_2$ is also different in that it has the unusual temperature dependence for the resistivity that occurs in TiS_2. Upon intercalation with Li, there is a large reduction of the resistivity, again confirming that electrons are transferred to the conduction band (Onuki *et al.*, 1982b; Klipstein and Friend, 1983b).

Weak anomalies appear in the transport properties of the Li intercalates of all the Hf and Zr diselenides and disulphides at low temperatures, and may be associated with structural distortions in the layer or more likely with ordering of the lithium atoms (Klipstein and Friend, 1983b). Berthier *et al.* (1980, 1981) have studied Li_xZrSe_2 as a function of x and have reported a phase transition at $x = 0.4$, which they interpret as a non-metal to metal transition. On the other hand, Onuki *et al.* (1982b) find metallic behaviour throughout the entire composition range. This discrepancy may be due to different stoichiometries in the two samples, or perhaps the transition observed at $x = 0.4$ is caused by some other mechanism.

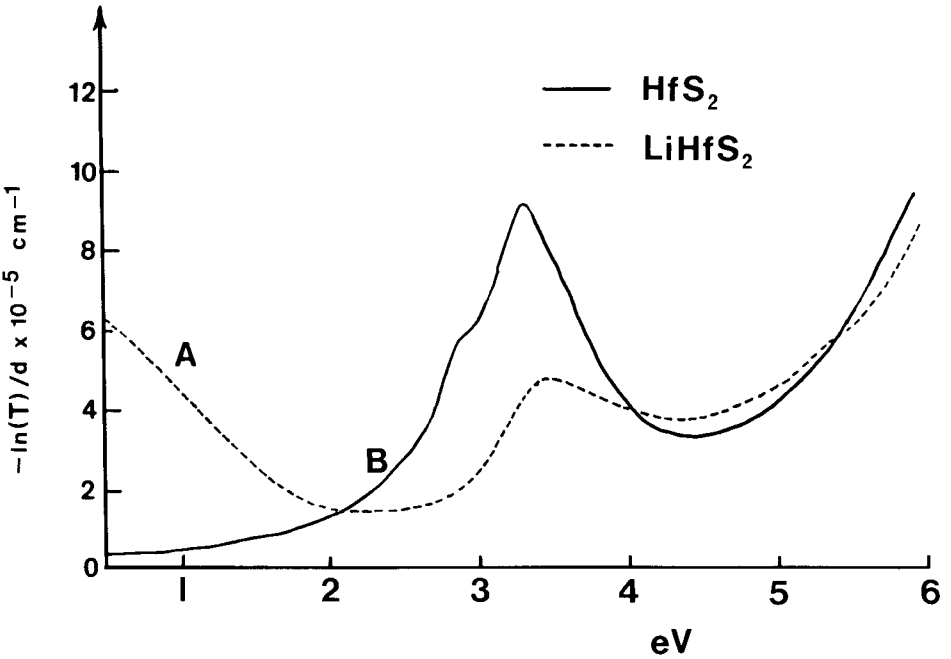

FIG. 11. Electronic absorption spectra of cleaved single crystals of HfS_2 at room temperature. Solid line: pure crystal; broken line: same crystal intercalated with Li to saturation limit (Beal and Nulsen, 1981a). 1 eV ~ 8000 cm^{-1}.

Sometimes, intercalation can cause a rearrangement of the layer stacking sequence of the host material. This is seen, for example, in Li_xZrS_2 and $NaTiSe_2$ (Rudorff, 1965; Whittingham and Gamble, 1975). This rearrangement involves a small adjustment of the chalcogenide layers from a hexagonal close-packed sequence (IT) to a cubic-type of close packing (3Ra), presumably as a result of repulsive forces between the intercalate ions, although $LiZrSe_2$ and $LiTiS_2$ do not show this change. The rearrangement has also been observed in the intercalation of ZrS_2 and $ZrSe_2$ with some of the Lewis bases, such as alkyl amines, pyridine, ammonia and hydrazine. Note, though, that the coordination of the Zr atom is not changed in this rearrangement *(Fig. 2)*. We saw earlier that trigonal prismatic coordination is stabilized by the occupation of the d_{z2} subband, and since intercalation of ZrS_2 involves addition of electrons to this band, we might expect a change of coordination as in the isoelectronic 2H–NbS_2. The intercalates, however, are formed at room temperature, and there is not enough energy for the sulphur atoms to rotate as much as the 60° necessary to achieve trigonal prismatic coordination (Yoffe, 1982). Fe_xZrSe_2, on the other hand, has been grown at 500–600°C and, for $x > 0.41$, it does have a trigonal prismatic structure (Gleizes *et al.*, 1976).

A series of M_xTS_2 complexes has been prepared where M = Fe, Co, Ni and Cu; T = Zr, Hf and $0 < x < 0.50$ (Trichet and Rouxel, 1969; Trichet *et al.*, 1972; Moreau *et al.*, 1975; Boswell *et al.*, 1979). X-ray and electron diffraction measurements of these compounds have indicated that the 1T structure is maintained in the host lattice and the intercalated ions occupy tetrahedral sites between the layers which, in some cases, are ordered at room temperature. Measurements at the absorption edge of the Ni, Fe and Cu intercalates of ZrS_2 showed a shift to lower energies (Yacobi *et al.*, 1979a,b), in sharp contrast to the optical results found for $LiZrS_2$, where intercalation caused a shift to higher energies due to electron

transfer. This is a surprising result, because it would imply that the rigid band model is not valid in this case, and so, at present, a departure such as this from the model remains a mystery. If it could be shown that some of the intercalate ions were present in intralayer sites, then the band structure might be modified in such a way as to give the observed change in the absorption edge. Self compensation between the intralayer and the interlayer 'guests' then might lead to semiconducting behaviour.

GROUP V

The most characteristic feature of the Group V disulphides and diselenides is their tendency to undergo structural distortions which are not related in a simple way to the underlying lattice — that is, they form incommensurate superlattices. This phenomenon is similar to the Jahn–Teller effect and is explained in these metallic materials as due to an intrinsic instability in the electron configuration of the conduction band, so that the incommensurability is related to details of electron correlation energies at the Fermi level. The instability manifests itself as an electron charge modulation, known as a charge density wave (CDW), and the ideal solid for such behaviour is one with a highly deformable positive ion background with strong electron–phonon (vibronic) interactions, since the effectiveness of the positive ion background depends on how strongly it is felt by the electrons (Overhauser, 1968). As a result of this interaction, the charge density wave is accompanied by a small change in crystal structure, known as a periodic lattice distortion (PLD). Obviously, for a distortion of this kind to occur, the gain in electronic energy must outweigh the energy required to deform the lattice. This energy difference depends on the number of electrons involved, the strength of the electron–phonon coupling and the frequency of the phonons involved. Relationships between these quantities have been derived which predict the conditions where CDW–PLD formation will be favoured (Chan and Heine, 1973; McMillan, 1975a; Doran, 1980; for reviews *see* Friedel, 1977; Friend and Jerome, 1979).

One important consequence of this theory is that the repeat unit of the structural superlattice is related directly to the wavelength (λ) of the charge density wave, so it may not be necessarily commensurate with the underlying lattice. For example, the superlattice reflection may be at $0.38\mathbf{a}^*$, where $\mathbf{a}^*$ is the reciprocal lattice vector of the underlying structure. This means that the wave vector q ($q = 2\pi/\lambda$) of the charge density wave is $0.38\mathbf{a}^*$. Another consequence of the theory is that conditions for a CDW–PLD are favoured in highly anisotropic systems, so it is not surprising that we find this phenomenon in the Group V dichalcogenides. The most direct evidence of a structural transition is, of course, from diffraction experiments, but the magnetic and transport properties of these materials are very sensitive to the distortion, and as a result, show anomalous behaviour at the transition temperature. The 2H polytypes, for example, have discontinuities in the slope of the resistivity–temperature curves, while the 1T polytypes have discontinuities in both slope and magnitude, often accompanied by temperature hysteresis.

Of the Group V materials that grow with the 1T structure, VSe_2, TaS_2 and $TaSe_2$ exhibit this CDW–PLD behaviour. 1T–VS_2 has been prepared but it is not known yet whether any distortion is present (Murphy *et al.*, 1977c). TaS_2 is unique in that it has two incommensurate phases. The $1T_1$ phase exists between 350 and 560 K, and has an incommensurate superlattice of $0.283\mathbf{a}^*$. Below 200 K in the $1T_3$ phase, there is a stronger distortion with the new lattice vector rotated away from the $\mathbf{a}^*$ direction by 13°54′, so that, in real space, a $3\mathbf{a} + \mathbf{b}$ commensurate superlattice is formed. Between 200 and 350 K there is a nearly commensurate phase $1T_2$, in which the superlattice is rotated most of the way towards the commensurate superstructure but is still incommensurate *(see Fig. 12)* (Williams *et al.*, 1974). The tendency towards commensurability (called lock-in) is the

driving force for the rotation of the superlattice in 1T–TaS_2, but it is probable that interlayer interactions favour the intermediate $1T_2$ phase and are necessary to stabilize it (Robbins and Marseglia, 1980). Certainly, we would expect intercalation to be a valuable probe for understanding the nature of these transitions as it will have an immediate effect on interlayer interactions.

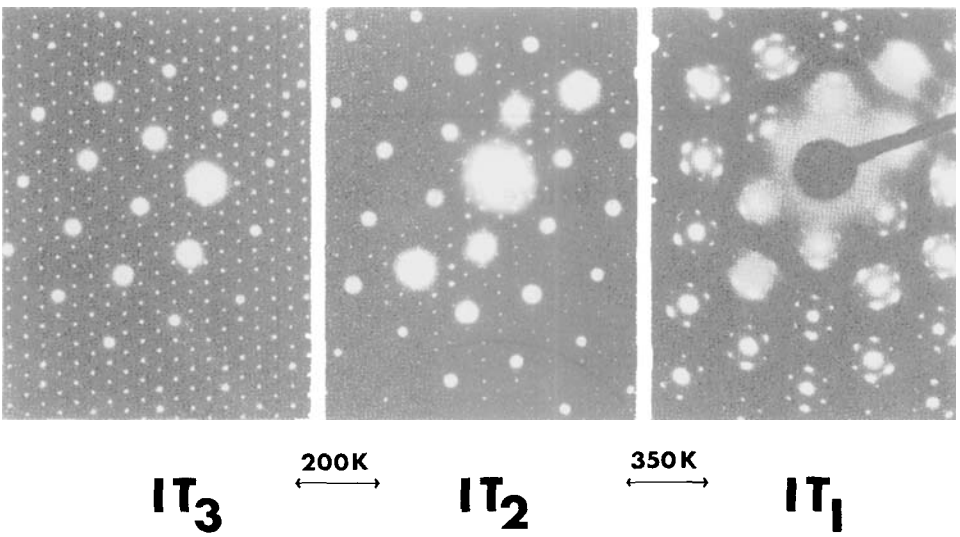

FIG. 12. Electron diffraction in TaS_2 (Williams *et al.*, (1974).

Another consequence of these charge-density-wave-induced distortions is to open up gaps in the Fermi surface which has the effect of reducing the number of free carriers in the conduction band. This is best understood by considering the effect on the band structure. *Figure 13* is a simplified scheme for a part of the d conduction band in 1T–TaS_2, showing energy plotted against the direction in reciprocal space which joins two adjacent electron pockets. The band is occupied up to the point where it crosses the Fermi level, and the electrons at this energy are free to move through the crystal. At the distortion temperature a new point of symmetry, and hence a superlattice reflection, is created at $0.283\mathbf{a}^*$. This causes gaps to appear in the band at the points marked A and B in *Figure 13a,* with the unoccupied part of the band shifting to higher energies and the occupied part shifting to energies below the Fermi level, E_F. The electrons below E_F are thus no longer free to move, and the overall number of carriers in the crystal is reduced — the stronger the distortion the bigger the gap, and hence, the more carriers removed. In spite of this reduction, there are still some carriers in parts of the band along other directions, and hence metallic behaviour can still be observed below the transition temperature. At very low temperatures (below 4 K) the few remaining conduction electrons in 1T–TaS_2 become localized by random potentials produced by defects in the crystal.

1T–$TaSe_2$ also exhibits strong distortions with atomic displacements of ~ 0.25 Å just as in TaS_2. The incommensurate phase exists from $\sim$ 600 K to 473 K, where it 'locks in' to the commensurate phase. The resistivity, however, remains metallic at all temperatures, showing no evidence for localization, perhaps because enough free carriers remain to screen out the localization potentials.

VSe_2 is different from the tantalum compounds in that it has an exceptionally narrow d_{z^2} band (Hughes *et al.*, 1980), which has the effect of reducing the tendency of CDW formation

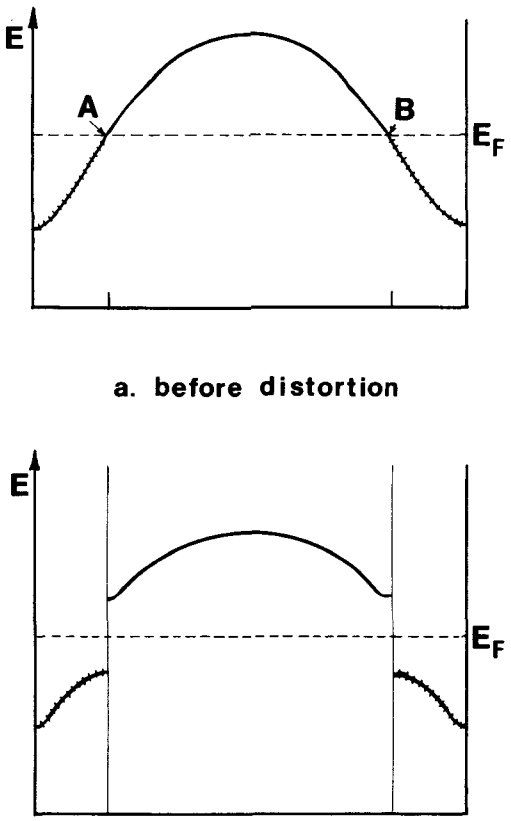

FIG. 13. Part of the d_{z^2} conduction band in 1T–TaS_2 plotted along the direction which joins two electron pockets. (a) Before the distortion, electrons at the Fermi level E_F are free to move. (b) After the distortion, gaps appear at A and B, the electrons are no longer at the Fermi level, and hence cannot contribute to the transport properties.

because of greater Coulomb repulsion (Friend *et al.*, 1978). In this case, the incommensurate transition occurs at 110 K and lock-in to a **4a** × **4b** commensurate superlattice occurs at 75 K (Williams, 1976), although other behaviour has also been reported and may be sensitive to sample quality (Di Salvo and Waszczak, 1981; Tsutsumi *et al.*, 1981). The CDW in VSe_2 is also different from that in other dichalcogenides, in that it is enhanced under hydrostatic pressure (Friend *et al.*, 1978). The main effect of pressure on the electronic structure of a solid is to increase the band width because of greater orbital overlap. This will have the effect of reducing the Coulomb repulsion between the electrons, and increasing the possibility of electron–phonon coupling. Both these effects favour the formation of charge-density waves.

Intercalates of 1T-tantalum dichalcogenides

1T–TaS_2 has been intercalated with the alkali metals, Li, Na and K, and electron diffraction studies where $x \sim 1/3$ and M = Na, K reveal a number of interesting superlattices that have

been associated with CDW–PLD distortions (Clarke and Williams, 1977). Thompson (1980) has found phase limits for Li_xTaS_2 at $x = 1/4$ and 6/7, using electrochemical methods, and has shown that for $x = 1/4$, there is a distortion of both the host and intercalate layers to a V_5S_8 type structure (see p. 197).

Further evidence for strong CDW–PLD transitions in intercalated 1T–TaS_2 comes from measurements on the hydrazine complexes $TaS_2(N_2H_4)_{4/3}$ and $TaS_2(N_2H_4)_{2/3}$ (Tatlock and Acrivos, 1978; Sarma *et al.*, 1982a). Both incommensurate and commensurate superstructures are found at room temperature and below 280 K, respectively, which have CDW wave vectors that are larger than in pure 1T–TaS_2 (from $\sim 0.283\mathbf{a}^*$ to $\sim 0.333\mathbf{a}^*$). This increase of $\sim$ 30% in wave vector is related to the increase in the size of the electron pockets as charge is transferred to the Ta d band*(see Fig. 6b).* In fact, the square of the CDW wave vector is roughly proportional to the number of electrons (Wilson *et al.*, 1975). Using this, and results from weight-gain measurements, it has been estimated that about ~ 0.3 electrons are transferred per TaS_2 unit for both complexes. At the same time though, we have seen that the distortion which accompanies the CDW has the effect of creating energy gaps at the Fermi level with the result that some electrons are no longer able to move through the conduction band. Hence, although a greater number of electrons are present due to charge transfer, the stronger CDW–PLD distortion in the intercalated material removes more carriers than in 1T–TaS_2. Clear evidence for this is seen in *Figure 14* in the resistivity curves for the two hydrazine complexes which show a much higher resistivity than the unintercalated TaS_2. Note also that there is a sharp rise in resistivity at low temperatures, indicating electron localization. In this 'localized' region the curve for the 4/3 complex has a temperature dependence of the form $\exp (T_0/T)^{1/3}$, where T_0 is related to the size of the localized wavefunction. This is the theoretically predicted behaviour for localized electrons in a two-dimensional random potential (Mott, 1974), where the electrons move by hopping from one localized site to another (variable range hopping). The random potential will be enhanced in these complexes by the random distribution of charged N_2H_4 ions. Further evidence for singly occupied localized states comes from the magnetic susceptibility which shows a Curie tail at low temperatures, and the presence of an ESR line in the same low temperature region (Guy *et al.*, 1982b). This hydrazine complex thus appears to offer a model example of a 'two-dimensional' system in which the theories for electron behaviour in localized states can be tested. Preliminary work has also been carried out on hydrazine intercalation of 1T–$TaSe_2$, and it appears that complexes similar to those in 1T–TaS_2 are formed, although the rise in resistance on cooling is much less, indicating weaker localization behaviour.

The ethylenediamine (EDA) intercalation complex of 1T–TaS_2, $(EDA)_{0.25}$ TaS_2, has been investigated by Meyer *et al.* (1975) who report an anomaly at 330 K in the resistivity curve which may indicate the same structural distortion as in 1T–TaS_2 at 350 K. However, from Raman and X-ray measurements on the same complex, Tsang and Shafer (1978) conclude that a commensurate superstructure is already present at room temperature, which they interpret as ordering of the EDA molecules between the layers. Clearly, more structural work is required to resolve this question.

Intercalates of 1T–vanadium dichalcogenides

The system Li_xVS_2 $(0 < x < 1)$ has two distinct distorted (monoclinic) phases for compositions near $x = 0.3$ and 0.5 which may be due to CDW–PLD distortions (Murphy *et al.*, 1977b). Above $\sim$ 85C the series becomes a single phase, and even at this temperature the hexagonal c/a ratio is abnormally high (1.85 for $Li_{0.5}VS_2$), an effect which is found in other materials with electronic instabilities. The c lattice parameter also goes through a maximum at $x = 0.5$, which suggests again that electronic effects due to the V conduction

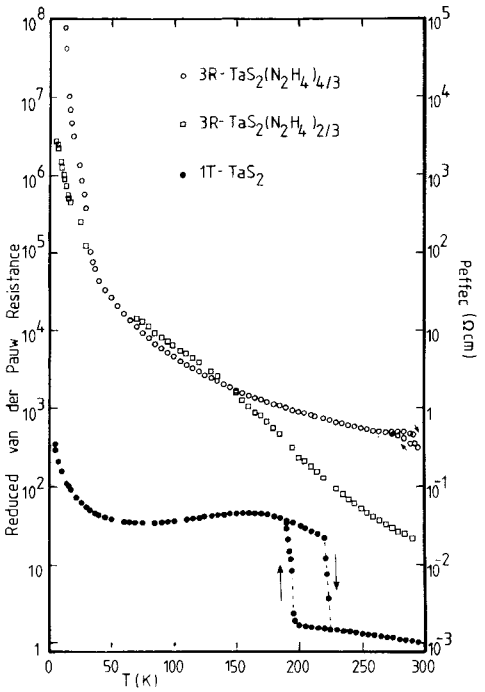

FIG. 14. Resistivity curves for 1T–TaS_2 and the two hydrazine intercalation complexes $3R_{I.I}$–$TaS_2(N_2H_4)_{4/3}$ and $3R_I$ – $TaS_2(N_2H_4)_{2/3}$ (Sarma *et al.*, 1982a).

band are more important than the size of the Li^+ ion in determining the lattice structure. This is also supported by experiments with the series $Li_xM_yV_{1-y}S_2$ (M = Fe or Cr), where the *c/a* ratios are reduced compared to the pure V compositions and there is less evidence for lattice distortions (Di Salvo *et al.*, 1979; Murphy *et al.*, 1979). Interestingly, electrochemical cells made with these compounds improve the reversibility of the Li_xVS_2 electrode, probably again due to the suppression of lattice distortions.

The lithium intercalates of VSe_2 have been investigated by several groups (Murphy *et al.*, 1976; Whittingham, 1978b; Murphy and Carides, 1979;, Thompson *et al.*, 1980). The phase diagram for Li_xVSe_2 suggests that there are three phases, each having a narrow range of stoichiometry, viz. $Li_{0.25}VSe_2$, $Li_{1.0}VSe_2$ and $Li_{2.0}VSe_2$. $Li_{0.25}VSe_2$ adopts a structure similar to the V_5S_8 ($V_{1/4}VS_2$) structure, with a distortion of the host layers (Thompson *et al.*, 1980). Transport measurements would be very helpful on this system to see whether or not the CDW distortions are strengthened in VSe_2 by lithium intercalation as they are by hydrazine intercalation.

An example of the effect of hydrazine is found in the complex $(N_2H_4)_{0.6}VSe_2$ (Sarma *et al.*, 1981). *Figure 15* shows the temperature dependent resistivity, where the anomaly at 110 K in unintercalated VSe_2 is seen to increase in magnitude and shift up to 165 K upon intercalation. This is a clear indication that a stronger distortion is present in the intercalated complex. The main effect of intercalation with hydrazine is, of course, the addition of electrons to the vanadium d band. Recalling that 0.3 electrons per TaS_2 formula unit are transferred in $TaS_2(N_2H_4)_{0.6}$ a similar increase in band filling is expected in VSe_2 $(N_2H_4)_{0.6}$. Hydrazine intercalation in VSe_2, therefore, has the same effect as hydrostatic pressure in that they both favour the formation of charge-density waves.

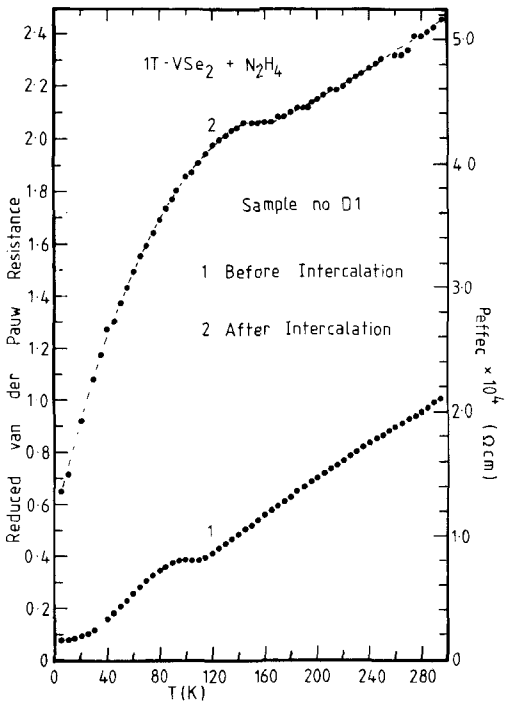

FIG. 15. Effective resistivity for VSe_2 before and after intercalation with hydrazine to form $VSe_2(N_2H_4)_{0.6}$ (Sarma *et al.*, 1981).

Unlike the Li and N_2H_4 intercalates, the systems Na_xVSe_2 and Na_xVS_2 show both semiconducting behaviour (Type II, $x = 1$) and metallic behaviour (Type I, $0.3 \lesssim x \leqslant 1$, for Na_xVS_2 and $0.5 \leqslant x \leqslant 0.6$, for Na_xVSe_2). The Type I compounds also have anomalous magnetic susceptibilities and transport properties, indicative again of some kind of phase transition (van Bruggen *et al.*, 1978). In contrast, the Type II $NaVS_2$ and $NaVSe_2$, which are semiconducting, have local moments on their V atoms which order antiferromagnetically at ~ 50 K. This ordering is accompanied by a first-order cooperative Jahn–Teller transition which leads to a monoclinic unit cell (van Bruggen *et al.*, 1978).

V_5S_8, or $V_{1/4}VS_2$, represents an interesting case of a self-intercalated transition metal dichalcogenide. The structure is often described as a metal deficient NiAs structure, but more relevant to us, it can be considered as a slightly distorted 1T structure with V atoms in the van der Waals gap, forming an ordered array with a $2\mathbf{a}$ superlattice. The ordering is slightly distorted so that the hexagonal c axis is inclined by 1.45° to the plane of the layers (Kawada *et al.*, 1975). Both NMR and magnetic susceptibility measurements have suggested a model in which the V atoms in the gap have a charge of +3 with 2 unpaired electrons which form local moments. These moments are then thought to be responsible for the antiferromagnetic transition at 28 K. The V atoms in the layer are considered to be non-magnetic because their electrons are delocalized and show metallic behaviour as we would expect for a $1T\text{–}3d^1$ TMDC (Silbernagel *et al.*, 1975). Recent neutron measurements indicate that some of the total moment of V_5S_8 resides on these intralayer V atoms (Forsyth *et al.*, 1979) perhaps as a result of a coupling interaction between the localized and delocalized electrons which we shall see evidence for later in the 2H-transition metal intercalates. It is also

possible to intercalate V_5S_8 with Li (Mercier *et al.*, 1979), in contrast to the self-intercalated $Ti_{1/3}TiS_2$, where Li intercalation has not been possible.

A polycrystalline sample of $P_{0.2}VS_2$ has been prepared by Ouvrard *et al.* (1982), which appears to be the first example of an electron acceptor intercalate in the transition metal dichalcogenides. The unit cell parameters show that the VS_2 sandwich layers have the 1T structure, but further detailed work is necessary before the exact positions of the P atoms and the physical properties are known. The closely related $P_{0.2}CrSe_2$ has also been synthesized by the same authors.

2H alkali metal intercalates

The Group V–2H materials exhibit both CDW–PLD distortions and superconductivity, and there has been a great deal of interest in the relationship between these two phenomena. Both require strong electron–phonon coupling which is found in all TMDCs, but superconductivity is favoured by a high density of electron states at the Fermi level whereas a CDW–PLD removes electron states from the conduction band. Thus, in the 1T materials, with strong charge-density waves, no superconductivity is observed. In the 2H materials, the distortions are much weaker, with only $\sim$ 10% of the average charge density involved. Hence a smaller number of carriers are removed at the transition and the remaining carriers do become superconducting at very low temperatures. Also, in the 2H compounds, the CDW distortion is removed by intercalation, so we expect a larger density of states at the Fermi level which favours superconductivity. This will lead to higher superconducting transition temperatures (T_c) in the intercalation complexes. For example, in 2H–TaS_2, T_c is at $\sim$ 0.6 K and increases to $\sim$ 4 K when it is intercalated with organic species (Thompson *et al.*, 1972; Meyer *et al.*, 1975). This increase also shows that superconductivity in these materials is essentially a two-dimensional effect, since the insertion of bulky molecules between the layers would certainly inhibit any normal layer–layer interactions (Coleman *et al.*, 1983).

The CDW–PLD distortion has been extensively studied in the 2H materials (Tidman *et al.*, 1974; McMillan 1975b, 1977; Moncton *et al.*, 1975, 1977; Berthier *et al.*, 1976, 1978; Stiles and Williams, 1976; Sugai *et al.*, 1981; Naito and Tanaka, 1982). $TaSe_2$ exhibits the strongest distortion in this group, with a transition to the incommensurate phase occuring at 122 K. At this temperature the incommensurate superlattice spacing is only fractionally different from 1/3 **a***, that is $(1-\delta)/3$ **a*** where $\delta \sim 0.03$. As the temperature is decreased, δ decreases continuously (but not to zero) until the lattice 'locks in' to 1/3 **a*** at 90 K. $NbSe_2$ has a similar but weaker transition pattern, the incommensurate phase appearing at 33 K, with $\delta = 0.03$. δ then decreases as the temperature is lowered until it reaches 0.01 at 5 K, but no lock-in transition has been observed below this temperature. Similarly 2H–TaS_2 shows no commensurate state down to 15 K.

It is not yet clear why the CDW–PLD transitions are weaker in the 2H polytypes. Recent theories have suggested that it may be due to the destruction of the long-range coherence of the charge-density wave, either through the phonon states or through strong scattering of the electronic states (Huntly *et al.*, 1978). It is also not well understood why intercalation suppresses the formation of CDW–PLDs in the 2H materials but again this may be due to changes in the phonons, which in turn would effect the electron–phonon interactions.

From the band scheme for the 2H structure and the rigid band model, we expect that intercalation of one atom of Li per TX_2 will completely fill the d_{z2} sub-band and so give semiconducting behaviour. This is found in $NbSe_2$, for example. *Figure 16* shows the optical transmission of $LiNbSe_2$, and the semiconductor $MoSe_2$, which is isoelectronic with $LiNbSe_2$. Note that there is little or no indication of the free carrier Drude edge in $LiNbSe_2$, and that at low photon energies, $LiNbSe_2$ and $MoSe_2$ have similar transmission curves,

although the excitonic features in $MoSe_2$, which are characteristic of a semiconductor, are not observed in $LiNbSe_2$ (Beal and Nulsen, 1981b). This may be because there are still a few carriers left which shield the weak potentials which would normally hold electron-hole pairs together as excitons. Differences in features at higher energies may be due to some involvement of the Li 2s and 2p bands in the optical transitions.

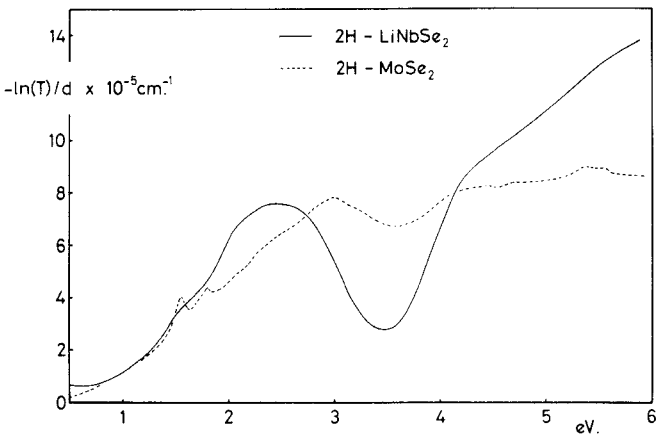

FIG. 16. Optical transmission for $LiNbSe_2$ and $MoSe_2$ (Beal and Nulsen, 1981b).

Some of the Na, K and Rb intercalates of the 2H TMDCs are listed in *Table 1,* which compares the increase in lattice parameters in these complexes upon intercalation. There does not seem to be a correlation between the increase in a axis and the size of the intercalate, or the amount of intercalate, but the fact that a increases at all can be explained qualitatively as follows. The length of the a axis is equivalent to the metal–metal bond distance within the layer, so it is this distance that is increased. Upon intercalation, electrons are transferred to the d sub-band of the transition metal *(see Fig. 5).* The hybrid orbitals in this band contain considerable d_{z^2} character as well as some $d_{x^2-y^2}$, d_{xy} and chalcogen p character, so that electron density will be increased both in the plane of the transition metal atoms and between coplanar chalcogen atoms. It is likely that this will lead to repulsion between neighbouring Nb atoms on the one hand and between coplanar Se atoms on the other, both effects tending to increase the a axis. Very little information is available on the effect of intercalation on the metal–chalcogen bond length. In VSe_2, intercalation with Na causes an increase in the V–V distance, with very little change in the V–Se distance (Wiegers, 1980), and similar results have been found for the hydrated compounds $K_{0.5}(H_2O)_yNbS_2$ and $K_{0.33}(H_2O)_yTaS_2$ (Graf *et al.,* 1979), and for $Rb_{0.28}NbSe_2$ (Bourdillon *et al.,* 1980). This suggests that the metal–chalcogen bond is little affected by charge transfer to the transition metal d band. Since it is the strongest bond in the crystal, the energy levels will lie in the valence band well below the Fermi level where the charge transfer is taking place. The fact that the lower-lying bands do not seem to be affected by this process lends further support to the rigid band approximation. It would be interesting to know the change in metal–chalcogen bond lengths in the Group IV lithium intercalates, because, as noted earlier, the a axis increases for $LiTiS_2$ and $LiTiSe_2$, but contracts in the case of the more ionic Zr and Hf disulphides and diselenides, perhaps suggesting some distortion of the TX_2 unit.

In concluding this section on the alkali metal complexes of 2H transition metal dichalcogenides, it is perhaps interesting to mention the rather special case of hydrogen intercalation. The hydrogen phases H_xTS_2 are known for T = Ti, Nb, Ta and $0 < x < 0.87$

TABLE 1. Increase in lattice parameters after alkali metal intercalation in some 2H layer compounds, measured by X-ray diffraction

	△a	△c	Ref
$Na_{0.67}NbSe_2$	0.026	2.826	a
$NaTaS_2$	0.02	2.49	a
$Na_{0.67}TaSe_2$	0.02	2.693	a
$Na_{0.3}MoS_2$	not refined	2.704	b
$K_{0.67}NbSe_2$	0.030	4.50	a
$K_{0.67}TaS_2$	0.017	4.40	a
$K_{0.67}TaSe_2$	0.033	4.34	a
$K_{0.4}MoS_2$	0.0433	4.286	b
$Rb_{0.28}NbSe_2$	0.029	4.58	c
$Rb_{0.56}NbSe_2$	0.029	5.13	c
$Rb_{0.3}MoS_2$	0.0436	4.899	b

(a) Omloo and Jellinek (1970)
(b) Somoano *et al.* (1973)
(c) Bourdillon *et al.* (1980)

(Murphy *et al.*, 1975), and transport and magnetic susceptibility measurements show that 1 electron per H atom is transferred to the d band of the host materials. In the system H_xTaS_2 and H_xNbSe_2 an enhancement of the superconductivity of the host was found for small values of x, similar to the effect we shall see in organic intercalates, and the same mechanism is thought to apply here, i.e., the suppression of the charge-density wave instability. Recent neutron measurements on the compounds $H_xTaS_2(x > 0.1)$ and $H_{0.76}NbS_2$ indicate that the protons do not reside between the sulphur layers as in the other intercalates but are in the plane of the Nb (Ta) atoms (Riekel *et al.*, 1979). The hydrogen is located at the centre of an equilateral triangle formed by three metal atoms, and is strongly bound to them with a bond length of 1.928(6) Å. This three-centre bond has only been established for $x > 0.1$, where the data also indicated ordering of the H atoms. The problem of the position of H for $x < 0.1$ is still not clear, and the possibility cannot be excluded that some hydrogen atoms are also present between the layers in this composition range.

2H organic intercalates

2H–TaS_2 has been the most widely studied of the TMDC for the intercalation of organic molecules because of the facility with which it accepts these guest species and the stability of the final product. Literally hundreds of organic and organo-metallic intercalates of TaS_2 are known, and although among them amines and other nitrogen containing materials are the most common guest species, a large class of intercalates can also be formed from phosphines and phosphine oxides (Subba Rao and Shafer, 1979; Schöllhorn, 1980; Jacobson, 1982).

Large bulky intercalates can cause quite considerable increases in layer separation, these increases being correlated to the molecular dimensions of the intercalate and the stoichiometry of the final product. For example, intercalation of 2H–TaS_2 with stearamide leads to a tenfold increase of the interlayer distance. In the *n*-alkylamine series $(C_nH_{2n+1}NH_2)TaS_2$, for $n = 1$ to 4, the c axis expansion is constant and the hydrocarbon chains lie parallel to the S layers. Eventually ($n = 11$–18) the parallel orientation gives way to a perpendicular orientation with a bilayer of two amine molecules end to end between each chalcogenide sandwich layer. For n between 5 and 11 there is a mixture of orientations and considerable disorder is observed (Gamble *et al.*, 1971). Apart from lattice parameter determinations, however, little is known about the detailed structures of these Lewis base intercalation compounds. Only for the cases of pyridine and ammonia has more detailed structural work been carried out.

In (pyridine)$_{1/2}TaS_2$ the stacking sequence of the TaS_2 layers changes from the $2H_a$ polytype to one which allows a staggering of the metal atoms *(see Fig. 17)* (Parry *et al.*, 1974). This may imply that the $2H_a$ structure is stabilized in the host material by interlayer metal–metal interactions which are lost upon intercalation. A more complicated effect of this kind has been seen in the Li_xNbS_2 system (McEwen and Sienko, 1982b) where changes in stacking sequence and superconductivity are sensitively dependent on values of x.

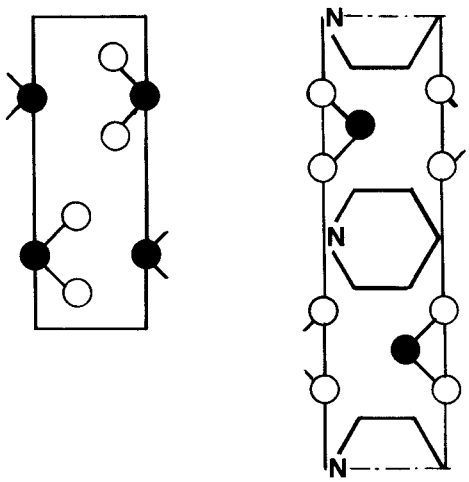

FIG. 17. 2H–TaS_2: (a) before intercalation, (b) after intercalation with pyridine. Pyridine has the same orientation in (pyridine)$_{1/2}NbS_2$.

Neutron diffraction experiments on (pyridine)$_{1/2}NbS_2$ have shown that the long CN axis of the pyridine molecule lies parallel to the dichalcogenide layers, and the nitrogen atom lies in the centre of the gap (*see Fig. 17*) (Wada *et al.*, 1978), giving a distance of 4.4 Å from the nitrogen atom to the nearest sulphur atom, a distance far too great for orbital overlap. Yet NMR and optical measurements indicate that a charge transfer of ~ 0.2 electrons to the Nb conduction band takes place (Ehrenfreund *et al.*, 1972; Beal and Liang, 1973b; Manzke *et al.*, 1981). So what is the bonding mechanism? Dines (1978) has suggested that back bonding may occur to empty π^* antibonding orbitals on the carbon atoms. Alternatively, there may be an electrostatic interaction between a positively charged organic cation and the negatively charged TMDC layer (Schöllhorn *et al.*, 1975, 1979; Riekel *et al.*, 1976). This requires the presence of H^+ during intercalation (0.25 H^+/mole TaS_2) and evolution of hydrogen gas in the deintercalation process, neither of which have been detected yet. A similar mechanism has been proposed in the case of ammonia intercalation, and evidence has been found here for the presence of small amounts of ammonium ions in the complex $(NH_3)TaS_2$ (Schöllhorn and Zagefka, 1977). It is argued that the nitrogen lone pairs are directed towards the ammonium ions, and the bonding is largely due to electrostatic interaction between the NH_4^+ ions and the negatively charged layers.

Although this model may be appropriate for NH_3 and pyridine intercalation, quite a different result is found in N_2H_4 complexes. Transport and magnetic measurements on the complex $TiSe_2(N_2H_4)_{0.6}$ have indicated a charge of + 0.75 on all the N_2H_4 molecules as a result of charge transfer (Sarma *et al.*, 1981; Guy *et al.*, 1982b). If hydrazinium ions were

present in this system, they would necessarily be highly concentrated, with such a large average hydrazinium charge. However, careful measurements on the hydrazine intercalation of both $TiSe_2$ and TaS_2 have failed to reveal any evidence for the presence of hydrazinium ions, or for the evolution of hydrogen upon deintercalation (Ghorayeb and Friend, 1983).

3d transition metal intercalates of the 2H TMDC

An interesting series of compounds is formed by the 3d transition metal intercalates of the 2H transition metal disulphides and diselenides, of formula M_xTX_2 (*see* Beal, 1979). The ordered complexes M = 3d transition metal; T = Nb, Ta; X = S, Se and $x = 1/4, 1/3$, have been studied extensively using transport, optical, magnetic and diffraction techniques (Friend *et al.*, 1977a; Parkin and Friend, 1980a,b,c; Parkin *et al.*, 1983a,b). In these materials the Nb or Ta atom has trigonal prismatic coordination within the sandwich layers and the 3d ions occupy octahedral sites between the layers *(see Fig. 18).* In the $x = 1/4$ complexes every fourth available octahedral hole is occupied giving rise to a **2a** superlattice and a structure with infinite M–T–M–T– chains perpendicular to the layers. In the $x = 1/3$ complexes, every third octahedral hole is occupied which gives rise to a $\sqrt{3}$**a** superlattice. In this structure the transition metal M is displaced in successive layers so that only three member chains of type T–M–T are formed along the *c* axis. The increase in *c* axis upon intercalation follows the expected variation due to the ionic radii of the transition metal ions.

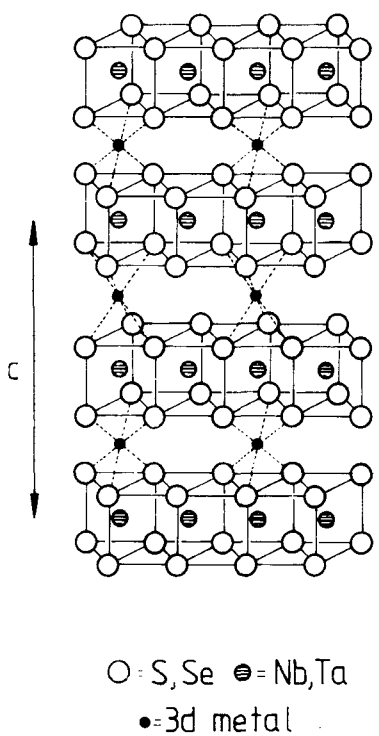

FIG. 18. Structure of the ¼ concentration 3d intercalation complexes of the 2H transition metal dichalcogenides.

These materials are not really intercalation complexes, in the sense that the ions in the van der Waals gap are not mobile and the structure is really strongly bonded in three dimensions. Also, the crystals have to be prepared from the elements rather than the 'guest' diffusing easily in and out of the 'host' at room temperatures. However, the guest metal ions do occupy interlayer sites and transfer electrons to the Nb or Ta d band, and many of the usual ideas for intercalation complexes, including the rigid band model, are still applicable. In fact, a number of different measurements have shown that the Nb or Ta d band structure remains little changed except for the filling of the d_{z^2} sub-band as a result of charge transfer (Friend *et al.*, 1977a; LeBlanc-Soreau *et al.*, 1976; Barry and Hughes, 1982). It has been found in these complexes that for M = V and Cr, the ions are trivalent and for M = Mn, Fe, Co and Ni, they are all divalent. Thus, for the $x = 1/3$ materials the d_{z^2} sub-band is either entirely filled (+ 3 complexes) or 5/6 filled (+ 2 complexes). This filling is evident from the position of the free carrier Drude edge, which is shifted to lower energies (Parkin and Beal, 1980) and from transport measurements, which show a decreased carrier concentration compared to the host materials (Parkin and Friend, 1980c). These latter measurements also show that both the CDW–PLD distortions and the superconductivity of the host lattices are totally destroyed by the presence of the 3d metal ions between the layers.

The most interesting feature of these complexes is that the remaining d electrons on the 3d metal ions are localized, since the ions are situated sufficiently far apart from each other between the layers that orbital overlap or band formation cannot take place. This formation of local moments leads to interesting magnetic and transport properties, some of which are summarized in *Table 2*. Note that all the complexes are metallic, even those where the d_{z^2} sub-band is meant to be filled (M^{+3}, $x = 1/3$). According to the rigid band model, if the d_{z^2} band is completely filled then we should expect semiconducting behaviour. This discrepancy may be due to slight deviations from 1/3 stoichiometry, or may be a slight change in orbital hybridization. That is, a small hybridization of d orbitals from the intercalate ion and d orbitals from the Nb or Ta ion could push the upper conduction band into the gap, or a broadening of the bands due to the increase in c axis may be enough to cause some d–d overlap. Either of these effects could lead to metallic behaviour.

TABLE 2. Magnetic transition temperature, type of order and room temperature Hall coefficient and electrical resistivity of the intercalation complexes, $M_{1/3}TaS_2$ and $M_{1/3}NbS_2$ (M = V, Cr, Mn, Fe, Co, Ni), $Mn_{1/4}TaS_2$ and $Fe_{1/4}NbSe_2$. F and AF correspond to ferromagnetic and antiferromagnetic orderings. The symbols ∥ and ⊥ give the direction of the easy axis of magnetization parallel and perpendicular to the c axis (Parkin and Friend, 1980a,b).

$M_{1/3}TaS_2$:	M = V	Cr	Mn	Fe	Ni	
Type of magnetic order	F⊥	F⊥	F⊥	F∥	AF	AF
Transition temperature (K)	35	116	70	35	35	120
Hall coefficient $R_H \times 10^3$ cm^{3}C^{-1}	3.2	2.6	1.0	0.6	0.83	0.82
Resistivity $\rho \times 10^4$ ohm cm	2.8	5.9	1.3	2.4	3.7	2.4

$M_{1/3}NbS_2$:	M = V	Cr	Mn	Fe	Co	Ni
Type of magnetic order	F⊥	F⊥	F⊥	AF∥	AF	AF
Transition temperature (K)	55	115	40	45	25	90
Hall coefficient $R_H \times 10^3$ cm^{3}C^{-1}	4.0	6.2	0.97	1.4	1.7	0.94
Resistivity $\rho \times 10^4$ ohm cm	3.0	11.6	1.5	3.2	3.5	2.2

	$Mn_{1/4}TaS_2$	$Fe_{1/4}NbSe_2$
Type of magnetic order	F⊥	AF∥
Transition temperature (K)	80	160
Hall coefficient $R_H \times 10^3$ cm^{3}C^{-1}	0.7	0.095
Resistivity $\rho \times 10^4$ ohm cm	1.9	2.9

Typical magnetic susceptibility results are shown in *Figure 19.* By orientating the crystals with *c* axes both parallel and perpendicular to the magnetic field it is possible to find the preferred orientation of the moment below the magnetic transition temperature. Above this temperature, in the paramagnetic regime, all of these systems, except the Fe complexes, have an isotropic susceptibility indicating that spin-only moments are present. The Fe complexes have anisotropic room temperature susceptibilities, showing that here there is an orbital contribution to the moments. The ferromagnetic iron complexes differ also in that the moment lies preferentially along the *c* axis, and at low temperatures $Fe_{1/3}TaS_2$, for example, is a hard ferromagnet with a large cohesive force (Eibshutz *et al.,* 1975). In the soft ferromagnets formed from the V,Cr and Mn complexes, the moments are in the plane of the layers.

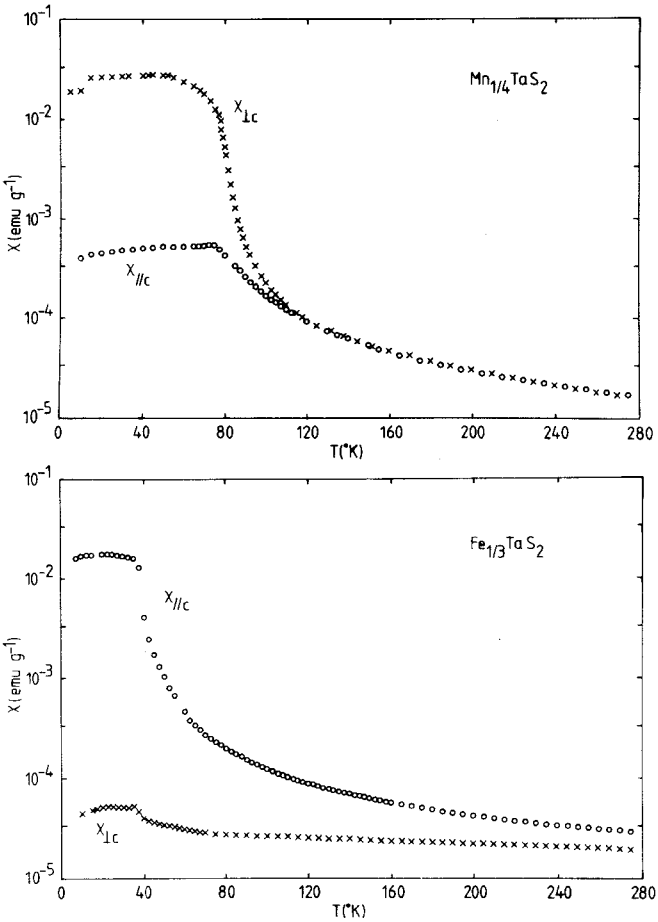

FIG. 19. Magnetic susceptibility of $Mn_{1/4}TaS_2$ and $Fe_{1/3}TaS_2$ both parallel and perpendicular to the *c* axis in a field of 330 gauss (Parkin and Friend, 1980a).

The Co, Ni and some Fe complexes order antiferromagnetically, and there is already some indication that a rich variety of magnetic structures form below the Neel temperature. Van Laar *et al.* (1971) have carried out powder neutron diffraction studies on $Fe_{1/3}NbS_2$ and $Cr_{1/4}NbS_2$ and have found two different magnetic structures. $Fe_{1/3}NbS_2$ adopts a complicated structure known as hexagonal ordering of the third kind, where the spin on each Fe ion is aligned antiparallel to 8 of its 12 nearest neighbours and parallel to the

remaining 4, and all spins lie perpendicular to the layers. $Cr_{1/4}NbS_2$ has a simpler structure in which ferromagnetic planes of Cr atoms are coupled antiferromagnetically along the c axis. A single crystal neutron diffraction study has recently been carried out on the antiferromagnet $Co_{1/3}NbS_2$, which has an unusual temperature dependence of the magnetization below T_N(25 K). A residual ferromagnetic moment develops along the c axis which depends on the magnetic field applied during cooling (Friend *et al.*, 1977a). Also, there appears to be a compensation temperature where the zero-field magnetization goes to zero (Parkin *et al.*, 1983a). Neutron measurements made at 4.2 K showed that the moments are similarly aligned to those in $Fe_{1/3}NbS_2$, except that they lie parallel to the layers (Parkin *et al.*, 1983a). Also, although the bulk of the magnetization is localized on the Co atoms there is some delocalization ($\sim$10%), perhaps as a result of hybridization between the Co 3d orbitals and the Nb 5d orbitals. We shall see that there is direct evidence for this type of interaction in $Mn_{1/4}TaS_2$. Further neutron work is now needed at temperatures closer to the Neel temperature to look for possible changes in this structure as a function of temperature, and for possible contributions from magnetic domains.

Preliminary neutron diffraction measurements have also been made on a single crystal of $Co_{1/3}TaS_2$, and it seems to have a very different magnetic structure (triangular antiferromagnetic) (Parkin *et al.*, 1983a). Chemically, $Co_{1/3}TaS_2$ and $Co_{1/3}NbS_2$ are very closely related. They have the same crystal structure and similar physical properties; thus, to have very different magnetic structures, the interactions between the moments on the Co ions in each compound must depend very critically on the unit cell size and, perhaps, on minor differences between the Nb and Ta d conduction bands, leading to differences in the interaction between the local moments and the conduction electrons.

A considerable body of evidence has now been accumulated which shows that a weak interaction of this kind does exist in these transition metal intercalates (Friend *et al.*, 1977a; Parkin and Beal, 1980; Parkin and Friend, 1980a,b,c; Parkin and Bayliss, 1982). This is seen, for example, in the magnetic susceptibility, the resistivity and the Hall coefficient as they are varied through the Neel temperature. *Figures 19 and 20* illustrate these anomalies in $Mn_{1/4}TaS_2$ and $Fe_{1/3}TaS_2$. Also, above the transition, there is an extra contribution to the electron scattering due to disordered spins, which is reduced below the Neel temperature as magnetic order builds up. This coupling between the local moments and the conduction electrons provides an obvious mechanism for the magnetic exchange interactions between the localized moments, direct exchange being ruled out by the large distances involved ($\sim$6 Å). The coupling mechanism, known as the RKKY interaction, causes conduction electrons near the localized moments to be spin polarized. The polarization is screened by the dielectric response of the conduction electron gas, and can lead to an oscillatory spin wave. Depending on the phase of the spin response at the next intercalate ion site, the effective coupling may be ferromagnetic or antiferromagnetic.

Direct evidence for this 3d–5d coupling mechanism, and confirmation that there is a local moment on the 3d ion comes from recent polarized neutron diffraction studies on the ferromagnet, $Mn_{1/4}TaS_2$ (Parkin *et al.*, 1983b). From the measured magnetic structure factors, a magnetic density distribution map of the unit cell was calculated. *Figure 21* shows the difference between this spin density and that calculated for the same structure, but with spherically symmetric $Mn^{+2}d^5$ ions. Two features are clear:

1. There is a distortion of the Mn^{+2} moment from spherical symmetry.
2. There is a net antiferromagnetic polarization around the Ta sites, with two distinct Ta sites.

The site with Mn immediately above and below must be where the initial spin polarization takes place and then the Ta atom in the second site is polarized in the opposite sense. This indirect antiferromagnetic coupling through the Ta atoms leads to overall ferromagnetic coupling of the spins on the Mn ions.

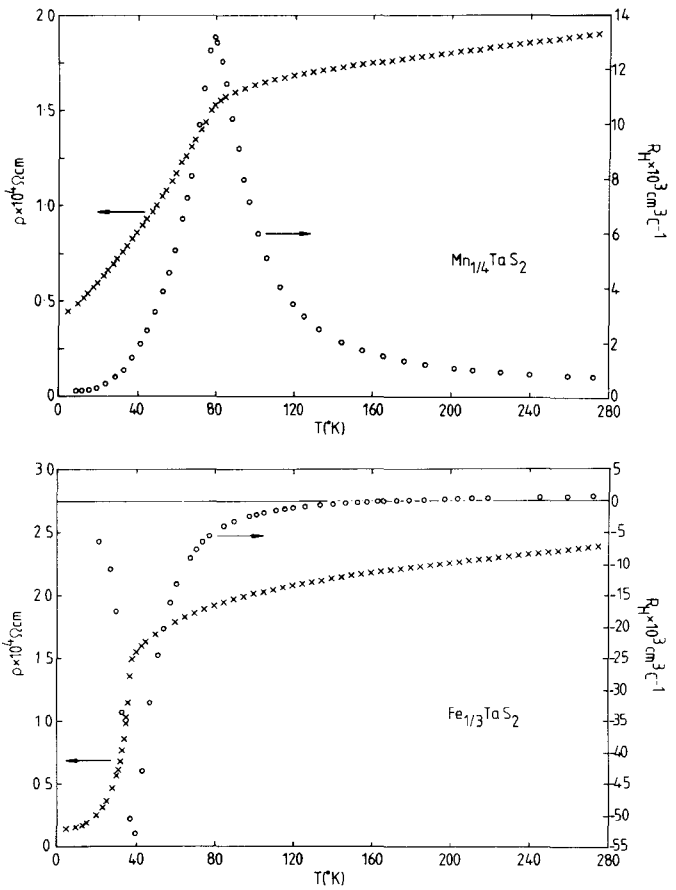

FIG. 20. Resistivity in the layers and Hall coefficient for current in the layers and magnetic field perpendicular to them in $Mn_{1/4}TaS_2$ and $Fe_{1/3}TaS_2$.

Studies have also been made on 3d transition metal intercalates of $NbSe_2$, $TaSe_2$ and TaS_2 where the intercalate ion is disordered. In these complexes, for $x < 0.3$, there is a very sensitive interplay between local moment formation on the 3d ions, suppression of the CDW distortions and the superconducting state, and the formation of spin density waves (Hillenius *et al.*, 1979). In the iron complexes, spin density waves have been found which condense at low temperatures to a novel kind of spin glass. Normally, a spin glass consists of localized magnetic moments situated on impurity atoms which are randomly distributed in a non-magnetic host. In the case of the iron intercalates, there is an interaction between the localized moments and the host (as we have already seen) and for disordered iron atoms, this leads to a random spin density wave in a nearly magnetic host. This system has been termed a 'spin density wave glass' (Antoniou, 1979). The essential feature of all types of spin glasses is that there is a sharp cusp in the curve of magnetic susceptibility versus temperature at the spin glass transition temperature, T_g, which is believed to arise from a competition between ferromagnetic and antiferromagnetic exchange interactions. In order to study the nature of this glass transition, Chen and Slichter (1983) have looked at the spin dynamics of the iron intercalate, Fe_xNbSe_2, using nuclear quadrupole resonance. In this system, spin glass samples are found at $x = 0.08$, 0.01 and 0.12, with transition temperatures at 4, 7.6 and 12 K respectively (Hillenius and Coleman,

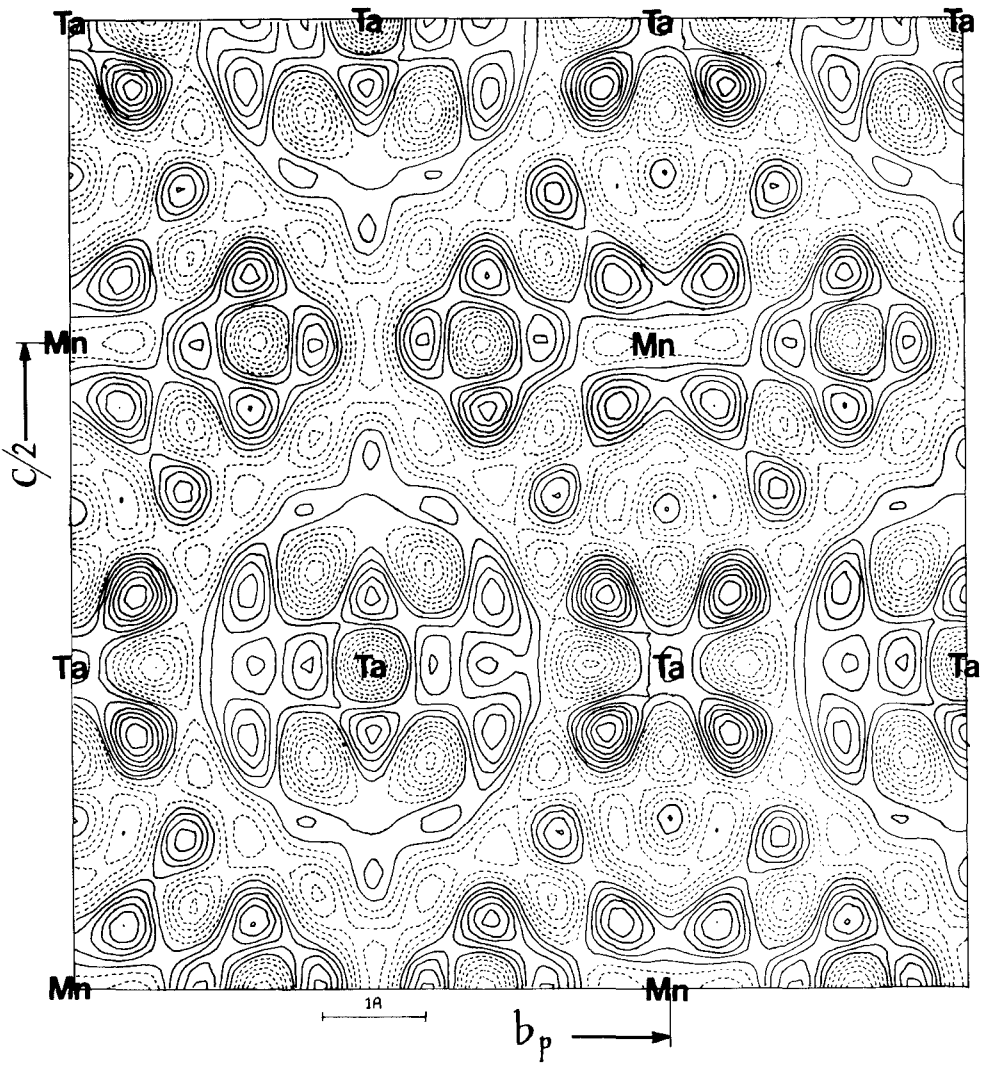

FIG. 21. Fourier difference map of the spin density $M^P_{obs} - M^P_{calc}$ for $Mn_{1/4}TaS_2$ projected along 100, where M_{calc} is the calculated moment arising from Mn^{+2} sites. Positive and negative contours are represented by full and dashed lines respectively, at intervals of $0.02\mu_B/1$ Å (Parkin *et al.*, 1983b).

1979). There are two theories about the nature of glass transitions and these can be extended to spin glasses as well. One views them as a genuine phase transition from one thermo-equilibrium state (paramagnetic in this case) to another (the spin glass state) (Edwards and Anderson, 1975). The other theory views the glassy state as a non-thermoequilibrium phase and the glass transition as a kinetic process (Tholence and Tournier, 1974). By looking at the relaxation rate of the spin autocorrelation function, Chen and Slichter were able to distinguish between these theories, and showed that their results were best described within the framework of the equilbrium phase transition theory.

2H post-transition metal intercalates

The 2H(Nb, Ta) dichalcogenides also form intercalation complexes with post-transition elements. The preparation, structures and some properties of Cu_xTX_2 and Ag_xTX_2 (T = Nb, Ta; X = S, Se) have been reported by Van Arkel and Crevecoeur (1963), Koerts (1963), Scholz and Frindt (1980; 1983) and Scholz *et al.* (1982). These compounds usually have Ag or Cu in tetrahedral holes between the TX_2 layers, and the stacking of the layers has changed from 2Ha to 2Hb. In $Ag_{0.6}TaS_2$, a second-order transition at 190K and a first-order transition at 96 K are observed from the behaviour of the lattice parameters and resistivity (*Figure 22*), and a $2\mathbf{a} \times 2\mathbf{b}$ superlattice is observed from electron microscope studies at low temperatures, indicating that at least one transition involves ordering of the Ag ions (Boebinger *et al.*, 1982). Weak anomalies have also been seen in resistivity vs T curves of Ag_xNbSe_2 complexes (Rogers, 1982). Compounds where M = Sn, Cd, Hg, Al, Ga, In, Ge, Sn, Pb and Tl have also been prepared, and preliminary structural investigations have shown that all the intercalate ions occupy octahedral sites within the van der Waals gap except Tl and In, which are in trigonal prismatic sites (Schmidt, 1971; Di Salvo *et al.*, 1973; Müller *et al.*, 1974; Eppinga and Wiegers, 1980). The Sn, Pb and Bi are ordered at room temperature, and surprisingly, the interatomic distances are comparable to those found in the pure metal. For example, the Sn–Sn distances in $SnTaS_2$ and Sn are 3.31 and 2.80 Å, and the Pb–Pb distances in $PbTaS_2$ and Pb are 3.33 and 3.50 Å, respectively (Eppinga and Wiegers, 1977). These distances allow the overlap of adjacent p_{xy} orbitals which can then broaden into a two-dimensional conduction band (Gossard *et al.*, 1974). Some question has arisen as to the charge on the Sn and Pb ions, since only one electron per intercalate ion is easily transferred to the host conduction band. $InTaS_2$ is known to adopt a similar structure, with almost identical lattice parameters, and in this case, In is most probably monovalent. Also, the Cu ion in Cu_xTaS_2 is thought to be monovalent (Di Salvo *et al.*, 1973). Monovalent Sn, however, seems less likely, and a model of a rapid valence fluctuation of Sn^0–Sn^{+2} has been proposed by Eppinga *et al.* (1981), based on the splitting of the Sn 3d peak in photoelectron spectroscopy (van de Berg and Cossee, 1968; Driscoll, 1978; Eppinga *et al.*, 1981). In $PbTaS_2$, the 4f photoelectron peak was broadened but no splitting was observed, perhaps indicating a faster exchange between the lead atoms. Charge fluctuation between Bi and Bi^{+3} has also been suggested for $Bi_{2/3}TX_2$ complexes (Eppinga and Wiegers, 1980).

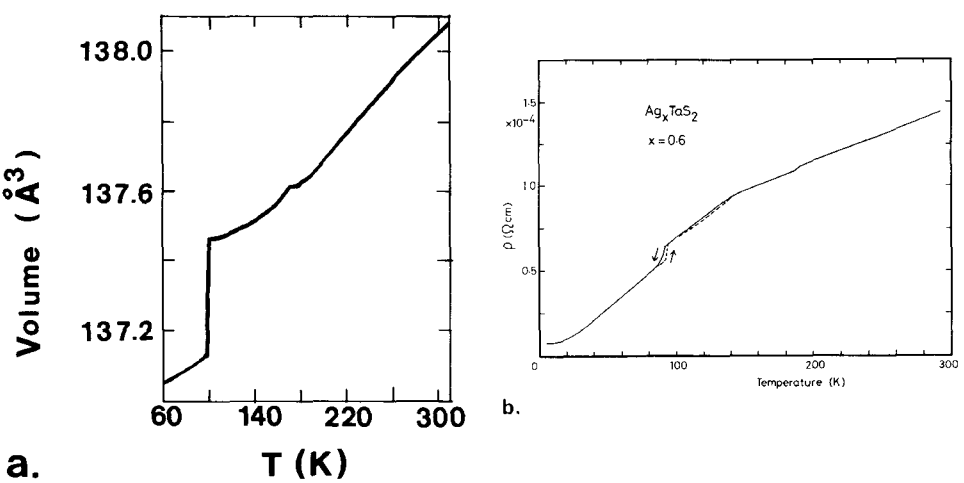

FIG. 22. Phase transitions in $Ag_{0.6}TaS_2$. (a) Unit cell volume versus temperature and (b) resistivity versus temperature.

The $x = 1/3$ Sn and Pb complexes are less complicated because in this case, the Nb or Ta d_{z2} sub-band can easily accommodate a transfer of 2 electrons per Sn(Pb) atom within the rigid band scheme and, as we would expect, transport data and photoelectron spectra are consistent with a charge of +2 on these ions (Eppinga *et al.*, 1981).

A generalized scheme for understanding the complicated superstructures observed in Cu_xNbS_2 and Cu_xTaS_2 complexes (De Ridder *et al.*, 1976; van Tendeloo *et al.*, 1977; van Goethem *et al.*, 1979) has been developed by De Ridder (1980). In particular, he has studied the partially disordered transition states where diffuse electron diffraction patterns are observed. His method, based on a kinematical theory, can be used to deduce possible predominant atomic configurations from the observed diffuse intensity contours.

GROUP VI

Intercalation of the Group VI 2H compounds occurs only for the most electropositive metals, since the electron affinity of the hosts is lower than that of the Group V hosts by about 1.5–2.0 eV (Thompson and Di Salvo, 1982). This of course, is due to the filled d_{z2} band which, in the rigid band model, requires any transfer of electrons to take place into the higher energy upper d bands (*see Figure 5*). As a result of this, we might expect to find that intercalation causes distortion of the host lattice, and, if there is enough energy available, we might expect a change to octahedral coordination (Yoffe, 1982; Py and Haering, 1983).

In fact, at room temperatures, most of the alkali metals can be intercalated into MoS_2 without changing the trigonal prismatic coordination of the host (Rudorff, 1965; Somoano *et al.*, 1973). However, the complexes are unstable, and it is necessary to use a solvent such as NH_3 which is also intercalated and which coordinates to and reduces the activity of the alkali metal — otherwise, disproportionation tends to occur, as in $LiMoS_2 \rightarrow Mo_{1.5} + \frac{1}{2}Li_2S$ (Whittingham and Gamble, 1975; however, see Py and Haering, 1983). A series of stable alkali metal intercalates with orthohombic symmetry has been prepared by reduction of MoS_2 at 700–900°C in which the MoS_2 layers are distorted (Schöllhorn *et al.*, 1978; Kümpers and Schöllhorn, 1980). Similarly, the iron intercalate $Fe_{1/2}MoS_2$ has been formed at high temperatures and here again the Mo atom has a distorted octahedral environment.

Optical transmission experiments on $NaMoS_2$ made from alkali metal ammonia solutions are shown in *Figure 23*, together with the transmission spectrum of the host material (Acrivos *et al.*, 1971). The sharp features marked A and B in MoS_2 are due to excitons which are characteristic of a semiconductor. From the figure we see that transfer of electrons from the intercalate to the conduction band causes the gradual disappearance of these excitons and the appearance of a free carrier Drude edge (C) indicating metallic behaviour as we would expect. Some of these alkali metal intercalates even become superconductors at very low temperatures. For example, $KMoS_2$ and $NaMoS_2$ have superconducting temperatures at 1.5 K and 4.5 K, respectively (Somoano and Rembaum, 1971).

Molybdenum disulphide is important technologically because of its widespread use as a catalyst in a number of reactions. These include, for example, hydrodesulphurization, and the isomerization and hydrogenation of olefins. Hence there is considerable interest in the reaction of H_2 with MoS_2 and the question of the role played by intercalation in catalytic processes.

Recently, a rather detailed study has been made on the uptake of hydrogen by polycrystalline MoS_2 at a number of different hydrogen pressures (Wright *et al.*, 1980; Sampson *et al.*, 1981; Sayers, 1981). Vibrational spectra, obtained from inelastic neutron scattering, have shown that at low pressures ($\sim H_{0.011}MoS_2$), the hydrogen atoms bond directly to single S atoms, perhaps those at the surface. At higher pressures, greater than 50 atm, a new peak appears in the vibration spectrum which has been associated with a different site for the

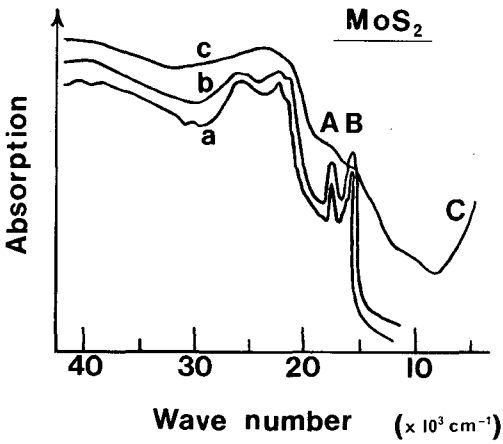

FIG. 23. Electronic absorption spectra of cleaved single crystals of MoS_2 at 77 K. (a) Pure crystal, (b) same crystal intercalated with Na (1 to 10% of saturation limit), (c) same crystal intercalated with Na to saturation limit. Curves have been vertically shifted to aid clarity (Acrivos *et al.*, 1971).

hydrogen atom, and there is a possibility this site may be in the van der Waals gap between the layers. This is supported by preliminary X-ray investigations which show that an extra Bragg peak appears in poorly crystalline MoS_2 after heating at 433 K in 1 atm of hydrogen. This peak corresponds to a new c axis lattice spacing of 15.6 Å, which is an increase of 3 Å over pure MoS_2. There is therefore enough space between the layers to accommodate two hydrogen atoms (Thomas *et al.*, 1977; Vasudevan *et al.*, 1982).

$CrSe_2$ and CrS_2

$CrSe_2$ is unique among the Group VI transition metal disulphides and diselenides in being the only one that has octahedral rather than trigonal prismatic coordination. The structure is of the $Cd(OH)_2$ type, with the Cr atoms in a trigonally distorted octahedral environment, and the material shows metallic properties with a strongly enhanced Pauli paramagnetism (Van Bruggen *et al.*, 1980). Band structure calculations suggest that it may be semi-metallic, like $TiSe_2$, with a partial overlap of the conduction d band with the valence p band (Myron, 1981). There is also evidence of a phase transition at 180 K. Experiments so far, however, have only been carried out on polycrystalline $CrSe_2$ and there are difficulties arising from its instability in air. To date, the sulphur analogue CrS_2 has not been prepared, but it is expected to be also unstable and have a similar structure.

The intercalates of CrS_2 and $CrSe_2$, $MCrX_2$ (M = Li, Ag, Cu, Na, K), are all stable at room temperature and have been known for some years (Bongers *et al.*, 1968; van Laar and Engelsman, 1973). Like $CrSe_2$, these compounds all have Cr atoms in a distorted octahedral environment, but now the d electrons are strongly localized on the Cr ions which are in the +3 valence state as a result of charge transfer from the intercalate ions. The materials are thus semiconductors, and a simplified band scheme, shown in *Figure 24*, places the localized levels in the gap between the p valence band and the empty conduction band formed from s orbitals on the Cr atom (Blazey and Rohrer, 1969; Khumalo and Hughes, 1980; Hughes *et al.*, 1981). The local moments on the Cr ions order antiferromagnetically and, with the exception of the Li complexes, the magnetic ordering consists of ferromagnetic layers (helical type for $NaCrS_2$) which lie perpendicular to the c axis and which couple antiferromagnetically to adjacent layers. The magnetic structure of $LiCrS_2$ is

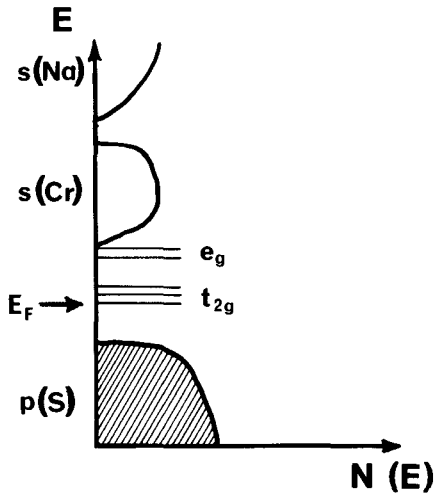

FIG. 24. Schematic band model for $NaCrS_2$ (after Khumalo and Hughes, 1980).

similar to that of $Fe_{1/3}NbS_2$ and $Co_{1/3}NbS_2$, consisting of a triangular arrangement of spins within the hexagonal planes and antiparallel coupling between adjacent planes.

In these materials all the alkali metals except K^+ are present in interlayer octahedral sites and the Ag^+ and Cu^+ ions are in tetrahedral sites (Bongers *et al.*, 1968). In K_xCrSe_2 ($0.6 \leqslant x \leqslant 0.8$), the K^+ ion occupies trigonal prismatic sites and the distance between the Cr atoms is much shorter (≈ 0.2 Å) than in $KCrSe_2$. There is also some evidence for the presence of both Cr^{+4} and Cr^{+3} ions (Eppinga and Wiegers, 1980).

A detailed X-ray structure analysis of $AgCrS_2$ has shed some light on the role of octahedral and tetrahedral sites in the ionic conduction of the Ag^+ ions (Hibma, 1982). At room temperature the silver ions are essentially ordered and occupy only one set of available tetrahedral sites. Above the order–disorder transition temperature (400°C), the silver ions are distributed over both sets of tetrahedral sites and the ionic conductivity is very high ($\sim 0.3\ \Omega^{-1}\ cm^{-1}$; Hibma, 1980a). Detailed electron density maps show that some silver ion density lies halfway between the tetrahedral sites, implying that some of the silver ions are in octahedral holes, presumably in off-site positions. This picture is corroborated by the nature of the diffuse X-ray scattering, which cannot be interpreted by considering substitutional disorder on tetrahedral sites alone.

CONCLUSION

We have seen that a large number of intercalation complexes can be formed from the transition metal disulphides and diselenides and that many of their properties can be qualitatively understood in terms of the simple rigid band model. In this model electrons are donated from the intercalate species to the d band of the host lattice with no further change in the overall electronic structure of the complex. A great deal of work still needs to be carried out to characterize these complexes even further and to explore in detail the interactions between the intercalate and the host lattice where more sophisticated models of the electronic and magnetic effects are required. The physics of these solids has only just begun to be investigated and it is likely that further studies will bring about a deeper understanding of these interesting and fascinating compounds.

ACKNOWLEDGEMENTS

I would like to thank A.D. Yoffe and R.H. Friend for their help and advice, and especially, I would like to express my appreciation to P.C. Klipstein for many useful and essential discussions, and for permission to include some of the results from his PhD dissertation.

REFERENCES

ACRIVOS, J. V. (1979). *Intercalated Layer Materials* (ed. F. Levy), p. 94. Dordrecht: Reidel.
ACRIVOS, J. V., LIANG, W. Y., WILSON, J. A. and YOFFE, A. D. (1971). *J. Phys. C., 4* L18.
ACRIVOS, J. V., PARKIN, S. S. P., CODE, J., REYNOLDS, J., HATHAWAY, K., KURASAKI, H. and MARSEGLIA, E. A. (1981). *J. Phys. C., 14,* L349.
ANDERSON, P. W. (1958). *Phys. Rev., 109,* 1492.
ANTONIOU, P. D. (1979). *Phys. Rev. B, 20,* 321.
BAGNALL, A. G., LIANG, W. Y., MARSEGLIA, E. A. and WELBER, B. (1980). *Physica, 99B,* 343.
BAGNALL, A. G., MARSEGLIA, E. A. and LIANG, W. Y. (1983). To be published.
BAK (1980). *Phys. Rev. Lett., 44,* 889.
BARRY, J. J. and HUGHES, H. P. (1982). *J. Phys. C., 15,* L797.
BARRY, J. J., HUGHES, H. P., KLIPSTEIN, P. C. and FRIEND, R. H. (1983). *J. Phys. C., 16,* 393.
BAYLISS, S. C. and LIANG, W. Y. (1982). *J. Phys. C., 15,* 1283.
BEAL, A. R. (1979). *Intercalated Layer Materials* (ed. F. Levy), p. 251. Dordrecht: Reidel.
BEAL, A. R. and LIANG, W. Y (1973a). *J. Phys. C., 6,* L482.
BEAL, A. R. and LIANG, W. Y. (1973b). *Phil Mag., 27,* 1397.
BEAL, A. R. and NULSEN, S. (1981a). *Phil Mag. B, 43,* 965.
BEAL, A. R. and NULSEN, S. (1981b). *Phil. Mag. B, 43,* 985.
BELL, M. G. and LIANG, W. Y. (1976). *Adv. Phys., 25,* 53.
BENESH, G. A., WOOLLEY, A. M. and UMRIGAR, C. J. (1983). To be published.
BERTHIER, C., CHABRE, Y. and SEGRANSAN, P. (1980). *Physica, 99B,* 107.
BERTHIER, C., CHABRE, Y., SEGRANSAN, P., CHEVALIER, P., TRICHET, L. and LE MEHAUTE, A. (1981). *Proc. Int. Conf. Semicond.,* Montpellier, France.
BERTHIER, C., JEROME, D. and MOLINIE, P. (1978). *J. Phys. C., 11,* 797.
BERTHIER, C., JEROME, D., MOLINIE, P. and ROUXEL, J. (1976). *Sol. St. Comm., 19,* 131.
BLAZEY, K. W. and ROHRER, H. (1969). *Phys. Rev., 185,* 71.
BOEBINGER, G. S., WAKEFIELD, N. I. F., MARSEGLIA, E. A., FRIEND, R. H. and TATLOCK, G. J. (1982). *Proc. Int. Conf. Semicond.,* Montpelier, France.
BONGERS, P. F., VAN BRUGGEN, C. F., KOOPSTRA, J., OMLOO, W. P. F., WIEGERS, A. and JELLINEK, F. (1968). *J. Phys. Chem. Sol., 29,* 977.
BOSWELL, F. W., YACOBI, B. G. and CORBETT, J. M. (1979). *Mat. Res. Bull., 14,* 1111.
BOURDILLON, A. J., PETTIFER, R. F. and MARSEGLIA, E. A. (1980). *Physica B, 99,* 64.
BROWN, B. E. (1966). *Acta Crystallogr., 20,* 268.
CHAN, S. K. and HEINE, V. (1973). *J. Phys. F, 3,* 795.
CHEN, C. H., FABIAN, W., BROWN, F. C., WOO, K. C., DAVIES, B., DeLONG, B. and THOMPSON, A. H. (1980). *Phys. Rev. B, 21,* 615.
CHEN, M. C. and SLICHTER, C. P. (1983). *Phys. Rev. B, 27,* 278.
CHIANELLI, R. R., SCANLON, J. C. and RAO, B. M. L. (1978). *J. Electrochem. Soc., 125,* 1563.
CLARK, W. B. (1976). *J. Phys. C., 9,* L693.
CLARKE, R., MARSEGLIA, E. and HUGHES, H. P. (1978). *Phil. Mag. B, 38,* 121.
CLARKE, W. B. and WILLIAMS, P. M. (1977). *Phil. Mag., 35,* 883.
COLEMAN, R. V., EISERMAN, G. K., HILLENIUS, S. J., MITCHELL, A. T. and VICENT, J. L. (1983). *Phys. Rev. B, 27,* 125.
CONROY, E. and PARK, K. C. (1968). *Inorg. Chem., 7,* 459.
DE RIDDER, R. (1980). *Physica B, 99,* 39.
DE RIDDER, R., VAN TENDELOO, G., VAN LANDUYT, J., VAN DYCK, D. and AMELINCKX, S. (1976). *Phys. Stat. Sol. (a), 37,* 591.

DINES, M. (1978). *Inorg. Chem., 17,* 763.
DI SALVO, F. J., EIBSCHUTZ, M., CROS, C., MURPHY, D. W. and WASZCZAK, J. W. (1979). *Phys. Rev., B, 19,* 3441.
DI SALVO, F. J., HULL, G. W., SCHWARZ, L. H., VOORHOEVE, J. M. and WASZCZAK, J. W. (1973). *J. Chem. Phys., 59,* 1922.
DI SALVO, F. J., MONCTON, D. E. and WASZCZAK, J. W. (1976). *Phys. Rev. B, 14,* 4321.
DI SALVO, F. J. and WASZCZAK, J. W. (1978). *Phys. Rev. B, 17,* 3801.
DI SALVO, F. J. and WASZCZAK, J. W. (1981). *Phys. Rev. B, 23,* 457.
DORAN, N. J. (1980). *Physica B, 99,* 227.
DRISCOLL, D. (1978). Dissertation, University of Fordham.
EDWARDS, S. F. and ANDERSON, P. W. (1975). *J. Phys. F, 5,* 965.
EDWARDS, J. and FRINDT, R. F. (1971). *J. Phys. Chem. Sol., 32,* 2217.
EHRENFREUND, E., GOSSARD, A. C. and GAMBLE, F. R. (1972). *Phys. Rev. B, 5,* 1708.
EIBSHUTZ, M., DI SALVO, F. J., HULL, S. W. and MAHAJAN, S. (1975). *Appl. Phys. Lett., 27,* 464.
ENGELSMAN, F. M. R., WIEGERS, G. A., JELLINEK, F. and VAN LAAR, B. (1973). *J. Sol. St. Chem., 6,* 574.
EPPINGA, R. and WIEGERS, G. A. (1977). *Mat. Res. Bull., 12,* 1057.
EPPINGA, R. and WIEGERS, G. A. (1980). *Physica B, 99,* 121.
EPPINGA, R., WEIGERS, G. A. and HAAS, C. (1981). *Physica B, 105,* 174.
FISCHER, J. E. and THOMPSON, T. E. (1978). *Phys. Today, 31,* 36.
FORSYTH, J. B., BROWN, P. J., KAWADA, I., NOZAKI, H. and SAEKI, M. (1979). *J. Phys. C., 12,* 4261.
FRIEDEL, J. (1977). *Electron–Phonon Interactions and Phase Transitions* (ed. T. Riste), p.1. New York: Plenum.
FRIEND, R. H., (1982). *Revue de Chimie Minerale, 19,* 467.
FRIEND, R. H. and JEROME, D. (1979). *J. Phys. C, 12,* 1441.
FRIEND, R. H., BEAL, A. R. and YOFFE, A. D. (1977a). *Phil. Mag., 35,* 1269.
FRIEND, R. H., JEROME, D., LIANG, W. Y., MIKKELSEN, J. C. and YOFFE, A. D. (1977b). *J. Phys. C., 10,* L705.
FRIEND, R. H., JEROME, D., SCHLEICH, D. M. and MOLINIE, P. (1978). *Sol. St. Commun., 27,* 169.
GABY, T. H., DE LONG, B., BROWN, F. C., KIRBY, R. and LEVY, F. (1981). *Sol. St. Commun., 39,* 1167.
GAMBLE, F. R. and GEBALLE, T. H. (1975). *Treatise on Solid State Chemistry* (ed. N.B. Hannay), vol. 3, New York: Plenum.
GAMBLE, F. R., OSIECKI, J. H., CAIS, M. and PISHARODY, R., (1971). *Science, 174,* 493.
GAMBLE, F. R. and SILBERNAGEL, B. G. (1975). *J. Chem Phys., 63,* 2544.
GHORAYEB, A. and FRIEND, R. H. (1983). To be published.
GLEIZES, A., REVELLI, J. and IBERS, J. A. (1976). *J. Sol. St. Chem., 17,* 363.
GOSSARD, A. C., DI SALVO, F. J. and YASUOKA, H. (1974). *Phys. Rev. B, 9,* 3965.
GRAF, H. A., LERF, A. and SCHÖLLHORN, R. (1979). *J. Less Common Met., 55,* 213.
GUY, D. R. P., FRIEND, R. H., JOHNSON, D. C. and SIENKO, M. J. (1982a). *J. Phys. C., 15,* L1251.
GUY, D. R. P., FRIEND, R. H., HARRISON, M. R., JOHNSON, D. C. and SIENKO, M. J. (1982b). *J. Phys. C, 15,* L1251.
HAAS, C. (1982). *The Physics of Intercalation Compounds* (ed L. Pietronero and E. Tosatti), p. 158. Berlin: Springer-Verlag.
HALLAK, H. A. and LEE, P. A. (1983). *Sol. St. Commun., 47,* 503.
HAMBOURGER, P. D. and DI SALVO, F. J. (1980). *Physica B, 99,* 173.
HIBMA, T. (1980a). *Sol. St. Commun., 33,* 445.
HIBMA, T. (1980b). *J. Sol. St. Chem., 34,* 97.
HIBMA, T. (1980c). *Physica B, 99,* 136.
HIBMA, T. (1982). *Intercalation Chemistry* (ed. M. S. Whittingham and A. J. Jacobson), p. 305. New York: Academic Press.
HILLENIUS, S. J. and COLEMAN, R. V. (1979). *Phys. Rev. B, 20,* 4569.
HILLENIUS, S. J., COLEMAN, R. V., DOMB, E. R. and SELLMEYER, D. J. (1979). *Phys. Rev. B, 19,* 4711.
HUGHES, H. P., PARKE, A. W., WILLIAMS, R. H. and BARRY, J. J. (1981). *J. Phys. C., 14,* L1103.
HUGHES, H. P., WEBB, C. and WILLIAMS, P. M. (1980). *J. Phys., C13,* 1125.
HUNTLEY, D. J., DI SALVO, F. J. and RICE, T. M. (1978). *J. Phys., C11,* L767.
JACOBSON, A. J. (1982). *Intercalation Chemistry* (ed. M. S. Whittingham and A. J. Jacobson), p. 229. New York: Academic Press.

KAWADA, I., NAKONO-ONODA, M., ISHII, M., SAEKI, M. and NAKAHIRA, M. (1975). *J. Sol. St. Chem., 15,* 246.
KHUMALO, F. S. and HUGHES, H. P. (1980). *Phys. Rev. B, 2,* 4066.
KLEINBERG, R. L., SILBERNAGEL, B. G. and THOMPSON, A. H. (1982). *Sol. St. Commun., 41,* 401.
KLIPSTEIN, P. C. (1982). PhD Dissertation, University of Cambridge.
KLIPSTEIN, P. C., BAGNALL, A. G., LIANG, W. Y., MARSEGLIA, E. A. and FRIEND, R. H (1981). *J. Phys., C14,* 4067–4081.
KLIPSTEIN, P. C. and FRIEND, R. H. (1983a,b). To be published.
KOERTS, H. (1963). *Acta Cryst., 16,* 432.
KÜMPERS, M. and SCHÖLLHORN, R. (1980). *Z. Naturforsch., B, 35,* 929.
LE BLANC-SOREAU, A., ROUXEL, J., GARDELTE, M. F. and GOROCHOV, O. (1976). *Mat. Res. Bull., 11,* 1061
LE NAGARD, N., GOROCHOV, O. and COLLIN, G. (1975). *Mat. Res. Bull., 10,* 1287.
LEVY, F. (1979). (ed.) *Intercalated Layer Materials.* Dordrecht: Reidel.
LOGOTHETIS, E. M., KAISER, W. J., KUKKONON, C. A., FAILE, S. P., COLELLA, R. and GAMBOLD, J. (1979). *J. Phys., C12,* L521.
MANZKE, R., CRECELIUS, G., FINK, J. and SCHÖLLHORN, R. (1981). *Sol. St. Commun., 40,* 103.
MATTHEISS, L. F., (1973). *Phys. Rev. B, 8,* 3719.
McCANNY, J. V. (1979). *J. Phys., C. 12,* 3263.
McEWEN, C. S. and SIENKO, M. J. (1982a). *Annales de Chimie, 7,* 433.
McEWEN, C. S. and SIENKO, M. J. (1982b). *Revue de Chim. Minerale, 19,* 309.
McMILLAN, W. L. (1975a). *Phys. Rev. B, 12,* 1187.
McMILLAN, W. L. (1975b). *Phys. Rev. B, 8,* 3719.
McMILLAN, W. L. (1977). *Phys. Rev. B, 16,* 643.
MERCIER, J., MASSENET, O., NGUYEN, V. D., DALARD, F., and FOULETIER, M. (1979). *Meeting of the French Chemical Society,* Paris, April, 1979 (unpublished).
MEYER, S. F., HOWARD, R. E., STEWART, G. R., ACRIVOS, J. V. and GEBALLE, T. H. (1975). *J. Chem. Phys., 62,* 4411.
MONCTON, D. E., AXE, J. D. and DI SALVO, F. J. (1975). *Phys. Rev. Lett., 34,* 734.
MONCTON, D. E., AXE, J. D. and DI SALVO, F. J. (1977). *Phys. Rev. B, 16,* 301.
MONCTON, D. E., DI SALVO, F. J. and AXE, J. D. (1978). *Proc. International Conference on Lattice Dynamics, Paris, 1977* (ed. M. Balkanski), p. 561. Flammarion Sciences.
MOREAU, C., SPIESSER, M. and ROUXEL, J. (1975). *C. R. Acad. Sci. Paris (Serie C), 280,* 1203.
MORET, R., HUBER, M. and COMES, R. (1977). *J. de Physique, 12,* C7, 202.
MORET, R., TRONE, E., HUBER, M. and COMES, R. (1978). *Phil. Mag.B, 38, 105.*
MOTT, N. F., (1974). *Metal–Insulator Transitions.* London: Taylor and Francis.
MÜLLER, D., POLTMANN, F. E. and HAHN, J. H. (1974). *Z. Anorg. Allg. Chemie, 410,* 129.
MURPHY, D. W. and CARIDES, J. N. (1979). *J. Electrochem. Soc., 126,* 349.
MURPHY, D. W., CARIDES, J. N., CROS, C., DI SALVO, F. J. and WASZCZAK, J, W, (1977a). *Mat. Res. Bull., 12,* 825.
MURPHY, D. W., CHRISTIAN, P. A. and CARIDES, J. N. (1977b). *J. Electrochemical Soc., 124,* 325.
MURPHY, D. W., CROS, C., DI SALVO, F. J. and WASZCZAK, J. W. (1977c). *Inorg. Chem., 16,* 3027.
MURPHY, D. W., DI SALVO, F. J. and CARIDES, J. N. (1979). *J. Sol. St. Chem., 29,* 339.
MURPHY, D. W., DI SALVO, F. J., HULL, G. W. and WASZCZAK, J. W. (1976). *Inorg. Chem., 15,* 17.
MURPHY, D. W., DI SALVO, F. J., HULL, G. W., MASCZAK, J. V., MEYER, S. F., STEWART, G. R., EARLY, S., ACRIVOS, J. V. and GEBALLE, T. H. (1975). *J. Chem. Phys., 62,* 967.
MYRON, H. W. (1981). *Physica B, 105,* 120.
NAITO, M. and TANAKA, S. (1982). *J. Phys. Soc. Jap., 51,* 219 and 228.
OMLOO, W. P. F. and JELLINEK, F. (1970). *J. Less Common Met., 20,* 121.
ONUKI, Y., INADA, R and TANUMA, S. (1982a). *J. Phys. Soc. Jap., 51,* 1223.
ONUKI, Y., INADA, R., TANUMA, S., YAMANAKA, S. and KAMIMURA, H. (1981). *Physica B, 108,* 1037.
ONUKI, Y., INADA, R., TANUMA, S., YAMANAKA, S. and KAMIMURA, H. (1982b). *J. Phys. Soc. Jap., 51,* 880.
OUVRARD, G., BREC, R. and ROUXEL, J. (1982). *Ann. Chim. Fr., 7,* 53–57.
OVERHAUSER, A. W. (1968). *Phys. Rev., 167,* 691.
PARKIN, S. S. P. (1983). Private communication.

PARKIN, S. S. P. and BAYLISS, S. C. (1982). *J. Phys., C15,* 6851.
PARKIN, S. S. P. and BEAL, A. R. (1980). *Phil. Mag. B, 42,* 627.
PARKIN, S. S. P. and FRIEND, R. H. (1980a). *Physica, 99B,* 219.
PARKIN, S. S. P. and FRIEND, R. H. (1980b,c). *Phil, Mag. B, 41,* 65; 95.
PARKIN, S. S. P., MARSEGLIA, E. A. and BROWN, P. J. (1983a). *J. Phys. C16,* 2765
PARKIN, S. S. P., MARSEGLIA, E. A. and BROWN, P. J. (1983b). *J. Phys. C16,* 2749.
PARRY, G. S., SCRUBY, C. B. and WILLIAMS, P. M. (1974). *Phil Mag., 29,* 601.
PIETRONERO, L. and TOSATTI, E. (1982). (eds) *The Physics of Intercalation Compounds.* Berlin: Springer-Verlag.
PY, M. A. and HAERING, R. R. (1983). *Can. J. Phys., 61,* 76.
RIEKEL, C., HOHLWEIN, D. and SCHÖLLHORN, R. (1976). *J. C. S. Chem. Commun.,* p. 863.
RIEKEL, C., REZNIK, H. G., SCHÖLLHORN, R. and WRIGHT, C. J. (1979). *J. Chem. Phys., 70,* 5203.
ROBBINS, M. O. and MARSEGLIA, E. A. (1980). *Phil. Mag. B., 42,* 705.
ROGERS, C. (1982). Private communication.
ROUXEL, J. (1980). *Physica, 99B,* 3–11.
ROUXEL, J., DANOT, M. and BICHAN, J. (1971). *Bull. Soc. Chim. Fr., 11,* 3930.
RUDORFF, W. (1965). *Chimia, 19,* 489.
SAMPSON, C., THOMAS, J. M., VASUDEVAN, S. and WRIGHT, C. J. (1981). *Bull. Soc. Chim. Belg., 90,* 1215.
SARMA, M., GHORAYEB, A., NULSEN, S. and FRIEND, R. H. (1981). *J. Phys., C14,* L1055.
SARMA, M., BEAL, A. R., NULSEN, S. and FRIEND, R. H. (1982a). *J. Phys., C15,* 477.
SARMA, M., BEAL, A. R., NULSEN, S. and FRIEND, R. H. (1982b). *J. Phys., C15,* 4367.
SAYERS, C. M. (1981). *J. Phys., C14,* 4969.
SCHMIDT, V. (1971). Dissertation, University of Tübingen.
SCHÖLLHORN, R. (1980). *Physica B, 99,* 89.
SCHÖLLHORN, R. (1982a). *Physics of Intercalation Compounds* (ed. L. Pietronero and E. Tosatti), p. 33. Berlin: Springer-Verlag.
SCHÖLLHORN, R. (1982b). *Intercalation Chemistry* (ed. M. S. Whittingham and A. J. Jacobson), p. 318. New York: Academic Press.
SCHÖLLHORN, R., ZAGEFKA, H. D., BUTZ, T. and LERF, A. (1979). *Mat. Res. Bull., 14,* 369.
SCHÖLLHORN, R., KÜMPERS, M. and PLORIN, D. (1978). *J. Less Common Met., 58,* 55.
SCHÖLLHORN, R., SICK, E. and LERF, A. (1975). *Mat. Res. Bull., 10,* 1005.
SCHÖLLHORN, R. and ZAGEFKA, H. D. (1977). *Angew. Chem., 89,* 193. (Eng. *16,* 199).
SCHOLZ, G. and FRINDT, R. F. (1980). *Mat. Res. Bull., 15,* 1703.
SCHOLZ, G. and FRINDT, R. F. (1983). *Can. J. Phys., 61,* 965.
SCHOLZ, G., FRINDT, R. F. and CURZON, A. E. (1982). *Phys. St. Sol. a, 71,* 531; *72,* 375.
SCHOLZ, G., JOENSEN, P., REYES, J. M. and FRINDT, R. F. (1980). *15th Conf. on Physics of Semiconductors,* Kyoto.
SILBERNAGEL, B. G., LEVY, R. B. and GAMBLE, F. R. (1975). *Phys. Rev. B, 11,* 4563.
SILBERNAGEL, B. G. and WHITTINGHAM, M. S. (1976). *J. Chem. Phys., 64,* 3670.
SOMOANO, R. B., HEDAK, V. and REMBAUM, A. (1973). *J. Chem. Phys., 58,* 697.
SOMOANO, R. B. and REMBAUM, A. (1971). *Phys. Rev. Lett., 27,* 402.
STILES, J. A. R and WILLIAMS, D. L. (1976). *J. Phys., C9,* 3941.
SUBBA RAO, G. V. and SHAFER, M. W. (1979). *Intercalated Layered Materials* (ed. F. Levy), p. 99. Dordrecht: Reidel.
SUGAI, S., MURASE, K., UCHIDA, S. and TANAKA, S. (1981). *Sol. St. Commun., 40,* 399.
SUTER, R. M., SHAFER, M. W., HORN, P. M. and DIMON, P. (1982). *Phys. Rev. B, 26,* 1495.
TAKEUCHI, S. and KATSUTA, H. (1970). *J. Jap. Inst. Met., 34,* 758. (in Japanese).
TATLOCK, G. J. and ACRIVOS, J. V. (1978). *Phil. Mag., 38,* 81.
TEMMERMAN, W., GLOTZEL, D., KELLY, P. and ANDERSON, O. K. (1982). CCP9 newsletter (Daresbury Laboratory) No. 2, p. 15.
THOLENCE, J. L. and TOURNIER, R. (1974). *J. Phys. (Paris), 35,* C4–229.
THOMAS, J. M., ADAMS, J. M., GRAHAM, S. H. and TENNAKOON, D. T. B. (1977). *Sol. St. Chem. of Energy Cons. and Storage, Adv. Chem. Series, 163,* 271.
THOMPSON, A. H. (1975a). *Phys. Rev. Lett., 34,* 520.
THOMPSON, A. H. (1975b). *Phys. Rev. Lett., 35,* 1786.

THOMPSON, A. H. (1978). *Phys. Rev. Lett., 40,* 1511.
THOMPSON, A. H. (1980). *Physica B, 99,* 100.
THOMPSON, A. H. and DI SALVO, F. J. (1982). *Intercalation Chemistry* (ed. M. S. Whittingham and A. J. Jacobson), p. 573. New York: Academic Press.
THOMPSON, A. H., GAMBLE, F. R. and KOCHLER, R. F. (1972). *Phys. Rev. B, 5,* 2811.
THOMPSON, A. H., GAMBLE, F. R. and SYMON, C. R. (1975). *Mat. Res. Bull., 10,* 915.
THOMPSON, A. H., SCANLON, J. C. and SYMON, C. R. (1980). *Sol. St. Ionics, 1,* 47.
TIDMAN, J. P., SINGH, O., CURZON, A. E. and FRINDT, R. F. (1974). *Phil. Mag., 30,* 1191.
TRICHET, L., COUSSEAU, J. and ROUXEL, J. (1972). *C. R. Acad. Sci. Paris. (Serie C), 274,* 394.
TRICHET, L. and ROUXEL, J. (1969). *C. R. Acad. Sci. Paris (Serie C), 269,* 1040.
TSANG, J. C. and SHAFER, M. W. (1978). *Sol. St. Commun., 25,* 999.
TSUTSUMI, K., SAMBONGI, T., TORIUMI, A. and TANAKA, S. (1981). *Physica B, 105,* 419.
UNGER, W. K., REYES, J. M., SINGH, O., CURZON, A. E., IRWIN, J. C. and FRINDT, R. F. (1978). *Sol. St. Commun., 28,* 109.
VAN ARKEL, A. E. and CREVECOEUR, C. (1963). *J. Less Common Met., 5,* 177.
VAN BRUGGEN, C. F., BLOEMBERGEN, J. R., BOS-ALBERINK, A. J. A. and WIEGERS, G. A. (1978). *J. Less. Common. Met., 60,* 259.
VAN BRUGGEN, C. F., HAANGE, R. J., WIEGERS, G. A. and DE BOER, D. K. G. (1980). *Physica B, 99,* 166.
VAN BRUGGEN, C. F., WIEGERS, G. A., HAANGE, R. J. and TOLSMA, (1979). *Coll. Abstr. VI Intern. Conf. Solid Compounds Trans. Elem.,* Stuttgart. p. 242.
VAN DER BERG, J. M. and COSSEE, P. (1968). *Inorg. Chim. Acta, 2,* 143.
VAN GOETHEM, L., DE RIDDER, R., VAN DYCK, D. and AMELINCKX, S. (1979). *Phys. Stat. Sol. (a),* 55, 67.
VAN LAAR, B. and ENGELSMAN, F. M. R. (1973). *J. Sol. St. Chem., 6,* 384.
VAN LAAR, B. and IJDO, D. J. W. (1971). *J. Sol. St. Chem., 3,* 590.
VAN LAAR, B., RIETVELD, H. M. and IJDO, D. J. (1971). *J. Sol. St. Chem., 3,* 154.
VAN TENDELOO, G., DE RIDDER, R., VAN GOETHEM, L., VAN DYCK, D., VAN LANDUYT, J. and AMELINCKX, S. (1977). *Phys. St. Sol.* (a), *42,* 319.
VASUDEVAN, S., THOMAS, J. M., WRIGHT, C. J. and SAMPSON, C. (1982). *J. Chem. Soc., Chem. Commun.,* p. 418.
WADA, S., ALLOUL, H. and MOLINIE, P. (1978). *J. Phys. Lett. (Orsay, Fr.) 39,* L243.
WHITTINGHAM, M. S. (1976). *J. Electrochem. Soc., 123,* 315.
WHITTINGHAM, M. S. (1978a). *Prog. Sol. St. Chem., 12,* 41.
WHITTINGHAM, M. S. (1978b). *Mat. Res. Bull., 13,* 959.
WHITTINGHAM, M. S. (1979). *J. Sol. St. Chem., 29,* 303.
WHITTINGHAM, M. S. and GAMBLE, F. R. (1975). *Mat. Res. Bull., 10,* 363.
WHITTINGHAM, M. S. and JACOBSON, A. J. (1982). (eds) *Intercalation Chemistry.* New York: Academic Press.
WHITTINGHAM, M. S. and THOMPSON, A. H. (1975). *J. Chem. Phys., 62,* 1588.
WIEGERS, G. A. (1980). *Physica B, 99,* 151.
WILLIAMS, P. M. (1976). *Physics and Chemistry of Materials with Layered Structures* (ed. F. Levy), vol. 2, p. 51. Dordrecht: Reidel.
WILLIAMS, P. M., PARRY, G. S. and SCRUBY, C. B. (1974). *Phil. Mag., 29,* 695.
WILSON, J. A. (1978a). *Phys. Rev. B 17,* 3880.
WILSON, J. A. (1978b). *Phys. Status Solidi. B, 81,* 11.
WILSON, J. A., DI SALVO, F. J. and MAHAJAN, S. (1975). *Adv. Phys., 24,* 117.
WILSON, J. A. and YOFFE, A. D. (1969). *Adv. Phys., 18,* 193.
WOO, K. C., BROWN, F. C., McMILLAN, W. L., MILLER, R. J., SCHAFFMAN, M. J. and SEARS, M. P. (1976). *Phys. Rev. B, 14,* 3242.
WRIGHT, C. J., SAMPSON, C., FRASER, D., MOYES, R. B. and RIEKEL, C. (1980). *J. C. S. Faraday I, 76,* 1585.
YACOBI, B. G., BOSWELL, F. W. and CORBETT, J. M. (1979a). *J. Phys., C12,* 2189.
YACOBI, B. G., BOSWELL, F. W. and CORBETT, J. M. (1979b). *Mat. Res. Bull., 14,* 1033.
YOFFE, A. D. (1982). *Ann. Chim. Fr., 7,* 215.